Kisspeptin fiber and receptor distribution analysis suggests its potential role in central sensorial processing and behavioral state control

Running title: Kiss1r and KP fiber mapping in rodent brain

Limei Zhang[1,2,*c], Vito S. Hernández[1,2,*c], Mario A. Zetter[1,5], Oscar R. Hernández-Pérez[1], Rafael Hernández-Gonzáles[6], Ignacio Camacho-Arroyo[7], Lee E. Eiden[2,c], Robert P. Millar[1,3,4]

[1]Dept. Physiology, School of Medicine, National Autonomous University of Mexico, Mexico City, Mexico
[2]Section on Molecular Neuroscience, NIMH-IRP, NIH, Bethesda, MD, USA
[3]Centre for Neuroendocrinology, University of Pretoria
[4]Dept. of Integrative Biomedical Sciences, Institute of Infectious Disease and Molecular Medicine, University of Cape Town, South Africa
[5]Department of Medicine and Health, University of La Salle, Mexico City, Mexico
[6]Vivarium, School of Medicine, National Autonomous University of Mexico, Mexico City, Mexico
[7]Research Unit in Human Reproduction, National Institute of Perinatology-Faculty of Chemistry, National Autonomous University of Mexico, Mexico City, Mexico
[*]These authors share first authorship.
[c] Correspondence: limei@unam.mx, vitohdez@unam.mx

Abstract

Kisspeptin (KP) signaling in the brain is defined by its anatomical framework, including the locations and chemotypes of KP-producing neurons, their fibers, receptors, and connections. Recent technological advances prompted us to re-evaluate these chemoanatomical aspects, initially studied during the early years following the discovery of KP and identification of its receptor. We recently characterized seven KP neuronal populations in the mouse brain using sensitive RNAscope methods, with two populations as new additions to the literature, and their short-term response to gonadectomy [(1)]. These results prompted us to continue in mapping KP fiber distribution in rats and mice and examined *Kiss1r* mRNA expression relative to that of the vesicular GABA transporter mRNA (*Slc32a1*), which provides a major chemoanatomical marker throughout the mouse brain. We identified KP fibers in 118 brain regions, predominantly in extra-hypothalamic areas involved in sensory processing and behavioral state control. Remarkably, KP fiber density was similar in aged long-term (one year) gonadectomized compared to intact mice, either male or female. *Kiss1r* was prominently expressed in brain sensory and state control regions, such as septal nuclei, tuberomammillary nuclei, the suprachiasmatic nucleus, the locus coeruleus, the hippocampal pyramidal and granule cell layers, the thalamic nuclei, and the cerebellar granule cell layer, as well as the interposed nucleus. *Kiss1r* was also co-expressed in *Kiss1*-expressing hypothalamic neurons and surrounding regions, suggesting autocrine and paracrine modes of KP action. These findings provide additional insight for further exploration of KP's role in brain control of complex physiological processes, independently of reproductive status.

key words: behavior state system, sensory-motor circuits, extrahypothalamic kisspeptin signaling, Kiss1r, autocrine

1. Introduction

Kisspeptin (KP) is a neuropeptide encoded by the *Kiss1* gene, initially known as metastin, identified via its role in inhibiting cancer metastasis [2]. It is now well-recognized as a critical regulator of the mammalian reproductive system, playing a pivotal role in the activation of the hypothalamo-pituitary-gonadal (HPG) axis by stimulating the release of gonadotropin-releasing hormone (GnRH) [3, 4]. Beyond its reproductive functions, KP is increasingly implicated in a variety of physiological processes, including the regulation of emotions and cognitive functions [5]. For instance, kisspeptin receptors are expressed in the amygdala, a critical region for emotional processing, and their activation has been associated with anxiolytic effects and the modulation of stress responses [6]. Additionally, KP has been implicated in cognitive functions such as learning and memory, potentially through its interactions with the hippocampus and prefrontal cortex [7]. These findings are supported by behavioral studies in animal models demonstrating that KP administration can enhance memory retention and reduce anxiety-like behavior [8] and modify fear response [9, 10]. As research continues to elucidate the molecular pathways and neural circuits involved, it has become increasingly clear that KP should play a multifaceted role in brain function, beyond reproductive function.

In a recent study in mouse, our group reported a comprehensive KP cell population description and molecular signature characterization within excitatory or inhibitory neurons throughout mouse brain, using a sensitive dual and multiple-channels in situ hybridization method. We described seven distinct KP populations, four of them within the hypothalamus and three of them as extrahypothalamic populations, two of which are newly-identified KP cell groups. Regulation of KP expression by short-term gonadectomy (GNX) was also reported quantitatively [1]. These results prompted us to extend the study by examining kisspeptin immunopositive fiber distribution in both rat and mouse, in comparison with KP receptor (Kiss1r) distribution using RNAscope methods.

There had been comprehensive anatomical studies on KP neuronal populations and fiber distributions in the brain of diverse animal species in the literature of the first decade after the discovery of KP, albeit hypothalamus and reproductive functions were the main focus of those studies, with less attention to KP expression in extrahypothalamic regions [11] [7, 12-14]. We examined KP fiber distributions in whole rat and mouse brain serial samples using a pan-specific KP antibody which recognizes the Kp decapeptide epitope within Kp-54, 14 and 10, with a less than 0.1% cross reactivity with other RF-amide peptides [15] and an immunohistochemistry procedure that maximizes staining sensitivity and reproducibility followed in our laboratories [16]. We report here 118 brain regions that contain KP fibers and terminals, with most of them located in extra-hypothalamic regions associated with central sensory processing and behavioral state control [17]. Surprisingly, the down-regulation of kisspeptin signaling from the rodent rostro-periventricular region (RP3V), observed after a short period of GNX in rodents reported previously by several groups including our own [1] was not evident in animals after long-term (12 months) GNX. Data from this study provide a new functional anatomical basis for further hypothesis generation and testing of the role of KP in a wider scope of brain function beyond reproductive function.

2. Results and focused discussion

2.1 Regional distribution of kisspeptin-expressing fibers and neurons in the mouse and rat brain

Due to the emerging evidence for kisspeptin function beyond its well-documented role in orchestration of GnRH secretion in the hypothalamus, it is imperative that reliable data concerning the comprehensive distribution of kisspeptin cell bodies and nerve fibers be obtained. At this time, there appear to be data sets that are reliable but incomplete, and some that, while comprehensive, have been questioned as potentially unreliable, due to adventitious cross-reactivity with other RF peptides. We have used a KP antibody with now well-documented authenticity and lack of cross-reactivity, and applied state-of-the-art tissue preparation and staining methods, in order to furnish a reliable and comprehensive description of the distribution of KP cell bodies and fibers throughout the brain contributing to a better understanding of the possible role(s) of KP first messenger function relevant to both reproductive and non-reproductive behavior beyond the regulation of GnRH secretion from the hypophysiotropic hypothalamus.

In this study, we performed KP-immunohistochemistry (IHC) using the pan-specific KP antibody which recognizes the KP decapeptide epitope within KP-54, 14 and 10, with a less than 0.1% cross reactivity with other RF-amide peptides [15] and an improved immunohistochemistry procedure followed in our laboratories [16], with picric acid added to the conventional fixative, strict time frames for fixation (15 min) followed by thorough washing, tissue slicing, and initiation of the IHC reaction immediately thereafter, coupled with long incubation with primary antibody (2 days at 4°C), to maximize the visualization of KP-positive fibers and neurons throughout the rodent brain. With this method, we observed greater intensity and a wider expression pattern of KP immunoreactivity in both mouse and rat brain than previously reported [11] [7, 12-14]. We found only one previous comprehensive report on the distribution of KP immunoreactivity in the rodent brain. In that study, authors used the antibody produced by Phoenix Pharmaceuticals [18] which has been cited as potentially cross-reactive with other RFRP peptides [12]. We have included the data reported by Brailoiu et al., [18] in rat, using the Phoenix Pharmaceuticals antibody anti-metastin (MT), in the table 1, with blue letters to facilitate comparison with the findings of the current investigation.

In table 1 (Tab. 1), we report 118 regions of the rodent brain in which we observed KP-ir labelling with differential strengths. When making detailed comparison with a previous publication [18], we found all the regions reported in this early study were replicated with our experiments. However, numerous new

Table 1. Distribution of kisspeptin immunoreactive (antibody GQ2) fiber distribution in mouse & rat brain with comparison of Brailoiu et al, JCN, 2005 (metastin, MT)

Structure	Abbr.	irMT cells (rat)	irGQ2 cells rat	irGQ2 cells mouse	irMT fibers (rat)	irGQ2 fiber rat	irGQ2 fiber mouse	Axons from RP3V viral tracers	Axons from Arc viral tracers
Telencephalon									
Cerebral cortex									
Cingular cortex	Cg		-	-		++	+		
Dorsal peduncular cortex	DP		-	-		++	+		
Dorsal tenia tecta	DTT		-	-		++	+	+	
Infralimbic cortex	IL		-	-		++	+		
Prelimbic cortex	PrL		-	-		++	+		
Ventral orbital cortex	VO		-	-		++	+		
Olfactory area									
Anterior olfactory nucleus	AON					++			+

Lat. septal n. ventral	LSV		-	-	++	+++	+++	+++	++
Medial septal nucleus	MS		-	-	+	+++	+	+	+
Septo-fimbrial n.	SFi		+	+		+	+	++	
Septo-hippocampal n.	SHi		+	+		+	+		
N. horizontal limb of the diagonal band	HDB		-	-	+	+	+	++	+
N. vertical limb of the diagonal band	VDB		-	-	+/-	+	+	+++	+
Diencephalon									
Hypothalamus									
Anteroventral periventricular n.	AVPe		+++	+++		+++	+++	+++	+++
Rostral periventricular area	RP3V		+++	+++		+++	+++		
Anterior hypothalamic area anterior	AHA		-	-		++	++	++	+++
Anterior hypothalamic area posterior	AHp		+	+	+	++	++		+++
Arcuate nucleus	Arc	+	++	++	+++	++++	++++	+++	++++
Dorsal hypothalamic	DH		++	++	+	+	+	+++	
Dorsomedial hypothalamic area	DM	+++	++	++	++	++	++	+++	++
Lat. hypothalamic area	LH		-	-	+	+	+	+	+
Lat. preoptic area	LPO		-	-	+	++	++	+++	
Medial preoptic area	MPA		-	-	+	++	++	+++	++
Median preoptic n.	MnPO		-	-	+	+++	+++	++++	+++
Parastrial nucleus	PS		-	-	+++	+++	+++		
Paraventricular hypothalamic n.	PVN	+	-	-	+	++	+	+++	+
Paraventricular hypothalamic n. medial magnocellular div	PVNmm		-	-		+++	+++	+++	+
Pa hypothalamic n. lateral magnocellular div.	PVNlm		-	-		+	+	+++	+
Pa hypothalamic n. lateral parvocellular div.	PVNmp		-	-		+++	+++	++	
Periventricular hypothalamic n. anterior	PVa		-	-		++	++		+++
Premammillary n. ventral	PMV		+	+		+++	++	+++	+++
Posterior hypothalamic area	PH		-	-	+	+	+	++	++
Retrochiasmatic area	RCh		-	-	+	+	+	++	++
Supraoptic nucleus	SON		-	-	+	++	++	+	
Tuber cinereum area	TC		-	-	+	++	+	++	
Ventral tuberomammillar n.	VTM		-	-		+++	++		+++
Ventromedial hypothalamic nucleus	VMH	+	-	-	+	+	+		+
Thalamus									
Anteromedial thalamic nucleus	AM		-	-		++	++		
Central medial thalamic nucleus	CM		-	-	+	+	+	++	
Mediodorsal thalamic nucleus	IMD		-	-	+	+	+		
Paratenial thalamic nucleus	PT		-	-	+	+	+		
Periventricular thalamic nucleus	PVT		-	-	+++	++++	++++	++	+
Reuniens thalamic nucleus	Re		-	-	+	+	+		
Rhomboid thalamic nucleus	Rh		-	-	+	+	+		
Submedius thalamic nucleus	SubD		-	-		+	+		
Zona incerta	ZI		-	-	+	+	+		
Epithalamus									
Habenular nucleus	Hb		-	-	++	++	++	+	
Mesencephalon									
Central nucleus of the inferior colliculus	CIC		-	-	+	++	++		

Cuneiform nucleus, dorsal part	CnFD		-	-		++	++		
Dorsal raphe nucleus	DR		-	-	+	++	++		
Deep mesenceph. n.	DpMe		-	-	+	+	+		
Interpeduncular n.	IP		-	-		+	+		
Median raphe n.	MnR		-	-	+	+	+		
Periaqueductal gray, lateral	LPAG		-	-		++	++	++	+
Periaqueductal gray dorsomedial	DMPAG	+/-	-	-	+++	+++	+++	++	+
Substantia nigra	SN		-	-	+	+	+		
Superior colliculus, intermediate and deep gray layer	DpG		-	-	+	+	+		
Supramammilary n.	SuM		-	-	+	+	++		
Ventral tegmental area	VTA		-	-		+	+	+	
Metencephalon and myelencephalon									
Ambiguus nucleus	Amb		-	-	+	+	+		
Area postrema	AP		+	+		+++	+++		
Caudoventrolateral reticular nucleus	CVL	+	-	-	+	++	++		
Dorsomedial tegmental area	DMTg		-	-		+	+		
Gigantocellular reticular nucleus	Gi		-	-	+	++	++		
Intermediate reticular nucleus	IRt		-	-	++	++	++		
Lateral parabrachial nucleus	LPB		-	-	+++	++++	++++	+	
Lateral reticular nucleus	LRt	+			++	++	++		
Lateral superior olive	LSO		-	-	++	+	+		
Locus coeruleus	LC		-	-	++	+++	+++	+	
Medial vestibular nucleus, magnocellular part	MVeMC		-	-	.	++	++		
Medioventral periolivary nucleus	MVPO		-	-		+++	+++		
Medullary reticular nucleus, dorsal part	MdD		-	-	+	++	++		
Medullary reticular nucleus, ventral part	MdV		-	-	+	+	+		
Nucleus of the solitary tract	Sol	+++	++	++	+++	++++	++++		
Parvicellular reticular nucleus	PCRt		-	-		++	++		
Parabrachial pigmented nucleus	PBP		-	-		+	+		
Pontine nuclei	Pn		-	-	+	-	-		
Pontine n, brachium pontis	bpPn		-	-		+	+		
Pontine raphe nucleus	PnR		-	-	+	-	-	+	
Pontine reticular nucleus, caudal part	PnC		-	-	+	+	+	++	
Pontine reticular nucleus, oral part	PnO		-	-	+	+	+	++	
Principal sensorial 5 n. dorsomedial	Pr5DM		-	-		++++	++++		
Raphe magnus nucleus	RMg		-	-	+	+	+		
Raphe obscurus nucleus	Rob		-	-	+	+	+		
Raphe pallidus nucleus	RPa		-	-	+	+	+		
Rostroventrolateral reticular nucleus	RVL	-	-	-	++	++	+		
Rubrospinal tract	rs	-	-	-	++	++	++		
Spinal trigeminal tract	Sp5	+	-	-	+++	-	-		
Spinal 3, gelatinous layer	Ge5		-	-		++++	+		
Superior cerebellar peduncle	scp		-	-		+++	+++		

Table caption: Distribution of kisspeptin immunoreactive (antibody GQ2) fiber distribution in mouse & rat brain with comparison of metastin, MT from Brailoiu et al, JCN, 2005 [18] in blue lettering. Semiquantitative annotations are used here: "-", not detectable; "+", weak; "++", low; "+++", moderate; "++++", intense; "+++++", very intense. Anatomical regions are ordered based on Brailoiu et al, JCN, 2005 modified based on Allen Institute Mouse Reference Atlas. Regions of rat, with higher density of KP fibers are highlighted in yellow. The two columns to the right are from analysis of two Kiss1-Cre mice injected Cre-dependent tracer in the arcuate nucleus (Arc, experiments 232311236 and 232310521) and two in the rostral periventricular region (R3PV, experiments 299247009 and 301989585) from the Allen Mouse Brain Connectivity Atlas.

In figure 1 we show KP immunohistochemical reactivity (-ir) in regions, including AVPV and VLPO where KP functions to regulate GnRH secretion, in comparison with other brain regions, with equally intense KP innervation, that are relevant in regulation of brain state, including MnPO, SHy, MS, LS and BST (panel A). Also depicted (Panel B), micrograph of a coronal section around Bregma -0.15mm, where 4 brain main conducting fiber systems can be clearly seen, i.e. the anterior commissure (ac), the stria medullaris (sm), the stria terminalis (st) and the fornix (f). KP-ir fibers running inside these conducting systems are indicated with red arrows. The dense innervation pattern of KP-ir fibers in the paraventricular anterior nucleus of the thalamus is shown. In panels C and D we show examples of KP-ir cell bodies and fibers in amygdalar complex. KP-ir fibers can be seen inside the stria terminalis (st), bed nucleus of stria terminalis, intra-amygdalar division (STIA), baso-medial amygdala (BMA), nu. basalis of Meynert (NBM) and medial amygdala (MEA). Some fibers within the medial amygdala, postero-dorsal division (MEApd), are observed coming from the stria terminalis, with main axons branching within the MEApd, of possible hypothalamic origin. In Tab 1, we summarize an analysis of experiments of two Kiss1-Cre mice injected Cre-dependent tracer in the arcuate nucleus (Arc, experiments 232311236 and 232310521) and two in the rostral periventricular region (R3PV, experiments 299247009 and 301989585) from the Allen Mouse Brain Connectivity Atlas. Fibers appear to reach amygdala via the stria terminalis (C1, red arrows). Panels Es and Fs show photomicrographs from the hypothalamic tuberal region, where the KP-ir cell bodies are seen in arcuate nucleus, and in premammillary nucleus, ventral division. KP-ir fibers are observed in other regions relevant for behavioral state control at this level, such as ventral, magnocelular and dorsal tubero mammillary nu., posterior hypothalamus, zona incerta (ZI) and subthalamic nu. (STN) Panel E2 shows the third ventricle at the level of Arc posterior. Abundant KP-ir fibers extended toward the lumen of the ventricle (also see the A3, red arrows). Panels G-K are micrographs of samples from parasagittal sections of mouse hindbrain. Panel G show the KP-ir cell bodies and dense KP-ir fibers in the solitary tract (sol) nu. (NTS) of mouse medulla. H and I show the dense innervation pattern of KP-ir fibers in pontine nuclei: lateral parabrachial nu. (LPBN) and locus coeruleus (LC) respectively. J and K show the dense KP-ir fibers in the spinal trigeminal tract (Sp5, K) and in the gelatinous layer of Sp5 (Ge5). Note that within the Ge5, the KP-ir fiber make perisomatic contacts with the cell bodies of the Ge5 (J, red arrows).

In Figure 2, we present chartings of mouse KP cell and fiber distribution. Panels A, B and C, (in register with [11] for purposes of comparison) show intense KP innervation of the prefrontal structures, such as cingular cortex (Cg), dorsal peduncular cortex (DP), dorsal tenia tecta (DTT), infralimbic cortex

170 (IL), prelimbic cortex (PrL), ventral orbital cortex (VO), nucleus accumbens shell (AcbSh), medial septal
171 nucleus (MS), nucleus of the diagonal band of Broca (NDB) and, dorsal division of the lateral septal
172 nucleus (LSd), which were not reported in the cited report. We also observed abundant innervation in
173 thalamic structures such as nucleus reuniens (Re), periventricular anterior nucleus (PVA) and the
174 epithalamic lateral habenula (LHb). In the amygdaloid complex, we observed KP fibers in cortico-
175 amygdala (CoA), nucleus of lateral olfactory tract (NLOT), the medial amygdala (MEA), mainly in the
176 postero-dorsal division, (MEApd), the basomedial amygdala (BLA) and the nu. of the stria terminalis,
177 intra-amygdala division (BSTIA) (Fig. 2, D-G). Midbrain and hindbrain sensory relay and state control
178 centers, such as premammillary nu. (PM), dorsal raphe nu. (DR), periaqueductal gray (PAG), subthalamic
179 nu. (STh) parabrachial complex (PBc), locus coeruleus (LC), Kölliker-Fuse nu. (KF) and nucleus of
180 solitary tract (NTS) are all seen with KP-ir fibers which were not reported previously (Fig. 2, H-L).
181

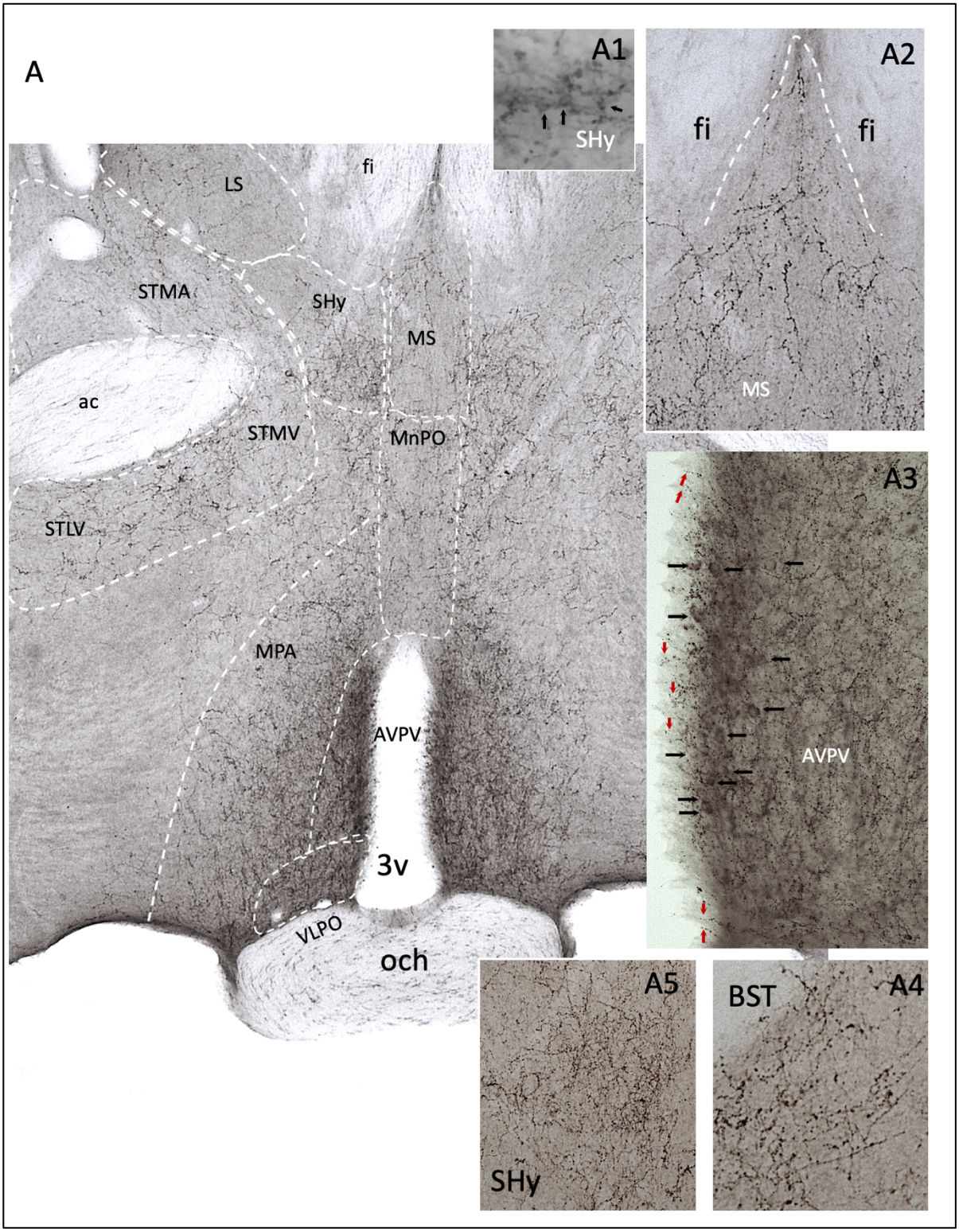

182
183
184
185
186

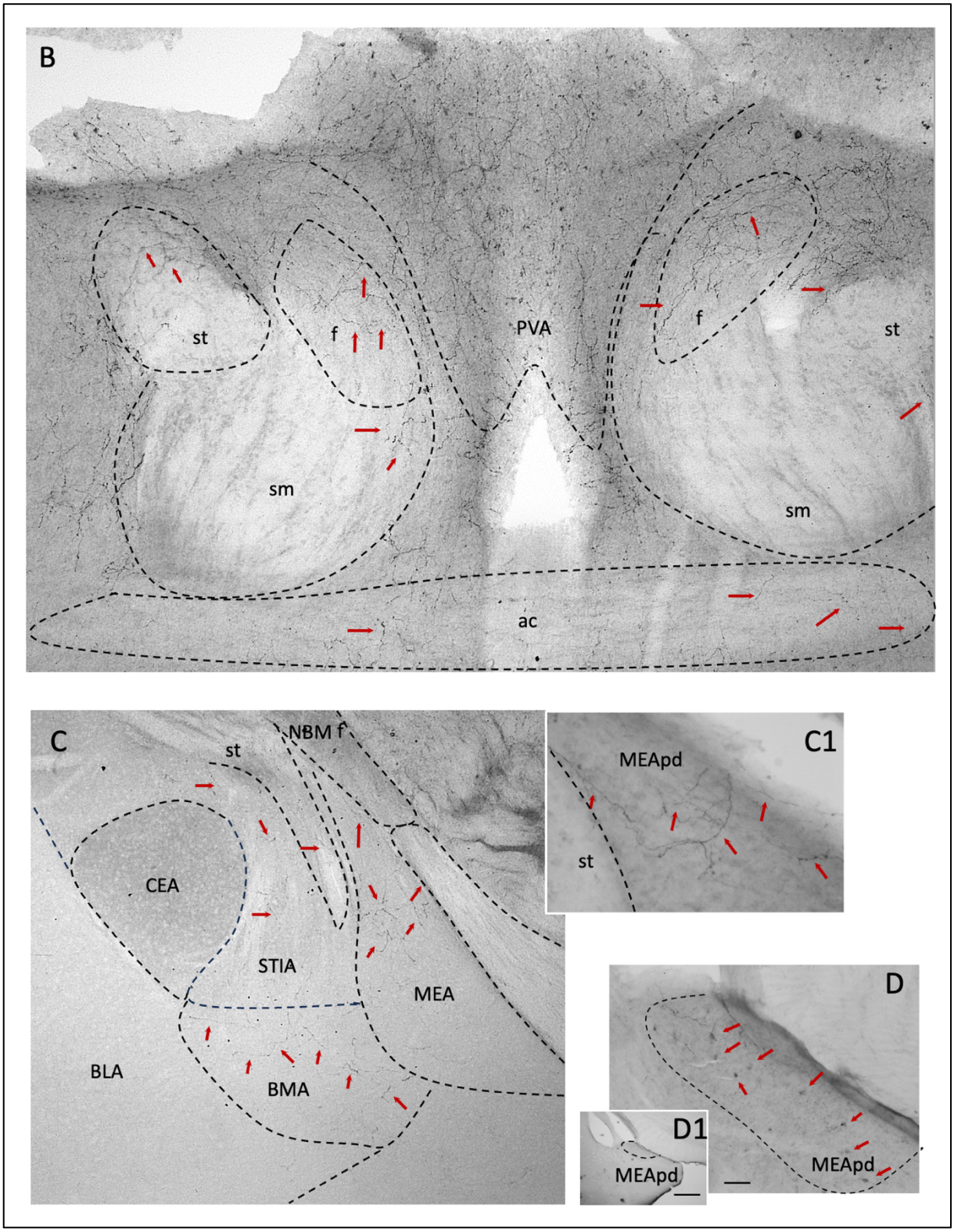
B
st
f
PVA
f
st
sm
sm
ac
C
NBM
st
CEA
STIA
MEA
BLA
BMA
C1
MEApd
st
D
D1
MEApd
MEApd

189

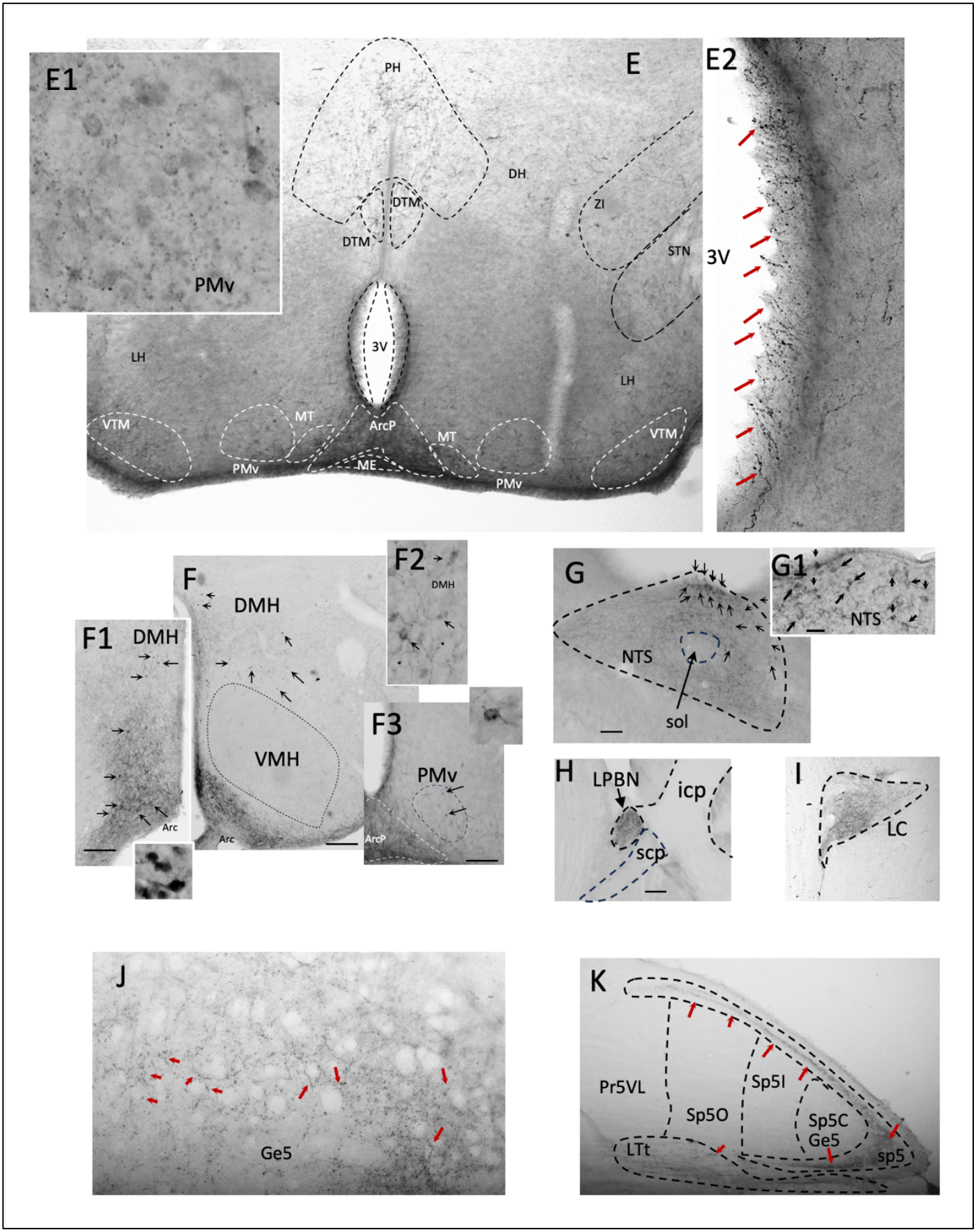
E1
PMv
E
PH
DH
DTM
DTM
ZI
STN
3V
LH
LH
VTM
MT
ArcP
MT
VTM
PMv
ME
PMv
E2
3V
F1
DMH
Arc
F
DMH
VMH
Arc
F2
DMH
F3
PMv
ArcP
G
NTS
sol
G1
NTS
H
LPBN
icp
scp
I
LC
J
Ge5
K
Pr5VL
Sp5I
Sp5O
Sp5C
Ge5
LTt
sp5

Fig. 1 KP immunohistochemical reactive (-ir) samples in mice using a polyclonal sheep anti-kisspeptin antibody [15] (GQ2, kindly supplied by Mohammad Ghatei†, Imperial College, London, UK), see Material and Methods section). This antibody recognizes kisspeptins 54, 14,13, and 10 that conserve the C-terminal decapeptide essential for biological activity and shows virtually no cross-reactivity (<0.01%) with other related human RF-amide peptides [15]. Panel A shows a low magnification micrograph at coronal plane (Bregma 0.38mm dorsal, 0.02 ventral [19]), where hypothalamic kisspeptinergic regions (regions containing KP-ir cell bodies, such as the antero-ventral periventricular nucleus (AVPV,A3), ventrolateral preoptic nucleus (VLPO) are shown. Besides, regions with high densities of KP innervation, which are relevant for brain state control, such as medial nucleus of preoptic area (MnPO), septo-hypothalamic nucleus (SHy, A1, A5, which also contains KP cell bodies, indicated with black arrows. For ISH image of SHy Kiss1 expressing neurons please see [1]), medial septal nucleus (MS, A2)), lateral Septal nu. (LS), bed nucleus of stria terminalis (BST, A4), with its subdivisions medio-anterior (STMA), medio-ventral (STMV) and latero-ventral (STLV). A3 shows the KP-ir in AVPV, where KP-ir neurons are indicated with black arrows and abundant KP-ir fibers innervating the ventricular surface are indicated with red arrows. Panel B, micrograph of a coronal section around Bregma -0.15mm, where 4 brain main conducting fiber systems can be clearly seen, i.e. the anterior commissure (ac), the stria medullaris (sm), the stria terminalis (st) and the fornix (f). KP-ir fibers running inside these conducting systems are indicated with red arrows. Also, the dense innervation pattern of KP-ir fibers in the paraventricular anterior nucleus of the thalamus is shown. Panel C shown a low magnification coronal micrograph of amygdala around the coordinate Bregma -1.58mm. KP-ir fibers can be seen in stria terminalis (st), bed nucleus of stria terminalis, intra-amygdalar division (STIA), baso-medial amygdala (BMA), nu. basalis of Meynert (NBM) and medial amygdala (MEA). Interestingly, some fibers within the medial amygdala, postero-dorsal division (MEApd), are observed coming from the st, that the main axon entered the MEApd and branched locally (C1, red arrows). Panel D shows a micrograph of MEApd at Bregma -2.18mm. Numerous KP-ir cell bodies are indicated with red arrows. D1 shows a lower magnification micrograph with the the circunscript region being the one of the panel D. Panels Es and Fs show the migrophotographs taken from the hypothalamic tuberal region, where the KP-ir cell bodies are seen in arcuate nucleus (Arc. E and F1), in Premammillary nucleus, ventral division (PMv, E and E1, F3, for ISH image of PMv Kiss1 expressing neurons please see [1]) and in the dorso-medial hypothalamic region (DMH, F, F1 and F2, black arrows). KP-ir fibers are observed in other regions relevant for behavioral state control at this level, such as ventral tuberomammillar nu. (VTM), magnocelular tuberomammillar nu. (MT) and dorsal tubero mammillary nu. (DTM), posterior hypothalamus (PH), zona incerta (ZI) and subthalamic nu. (STN) (E). E2 shows the third ventricle at the level of Arc posterior. Abundant KP-ir fibers extended toward the lumen of the ventricle (red arrows).Panel Gs- K are micrographs of samples from parasagittal sections of mouse hindbrain. Gs show the KP-ir cell bodies and dense KP-ir fibers in the solitary tract (sol) nu. (NTS) of mouse medulla. H and I show the dense innervation pattern of KP-ir fibers in pontine nuclei: lateral parabrachial nu. (LPBN) and locus coeruleus (LC) respectively. J and K show the dense KP-ir fibers in the spinal trigeminal tract (Sp5, K) and in the gelatinous layer of Sp5 (Ge5). Note that within the Ge5, the KP-ir fiber make perisomatic contacts with the cell bodies of the Ge5 (J, red arrows).

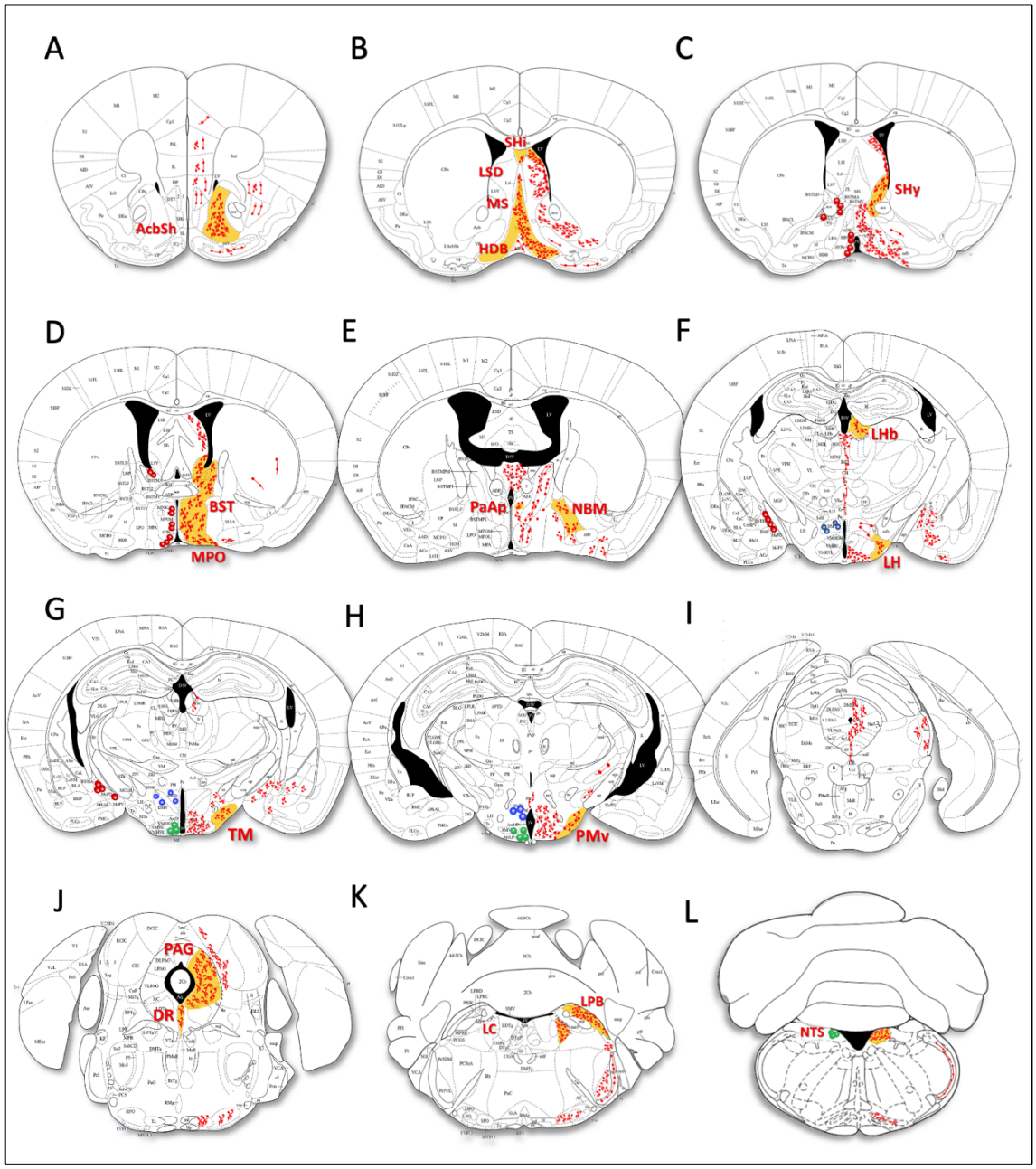

-

Fig. 2 Charting to represent the distribution of kisspeptin immunoreactivity in mouse brain. Sequential atlas planes show in the left side, KP immunoreactive cell bodies from the seven KP cell populations. Color-filled circles symbolizing the molecular signature previously reported [(1)]: KP-glutamatergic (green), KP-GABAergic (red) and expressing both VGluT2 and VGAT (blue). The distribution of KP-ir fibres are represented by red lines in the right hemisphere (the thickness of the lines has been exaggerated to ensure that the lines can be seen on the atlas planes). KP-ir fibers observed in brain areas relevant for behavioral state control are shaded in yellow: accumbens nucleus, shell (AcbSh), septohippocampal nu. (SHi), lateral septal nu. dorsal (LSD), medial septal nu. (MS), horizontal division of nucleus of dianogal band of Broca (HDB), septohypothalamic nucleus (SHy), bed nucleus of stria terminalis (BST), medial preoptic area (MPO), paraventricular anterior parvicellular division (PaAP), nucleus basalis of Meynert (NBM), lateral habenula (LHb), lateral hypothalamus (LH), tuberomammillary nu. (TM), ventral Premammillary nu. (PMv), periaqueductal grey (PAG), dorsal raphe nu. (DR), locus coeruleus (LC), lateral parabrachial nu. (LPB), nu. of solitary tract (NTS). See table 1 for rest of abbreviations.

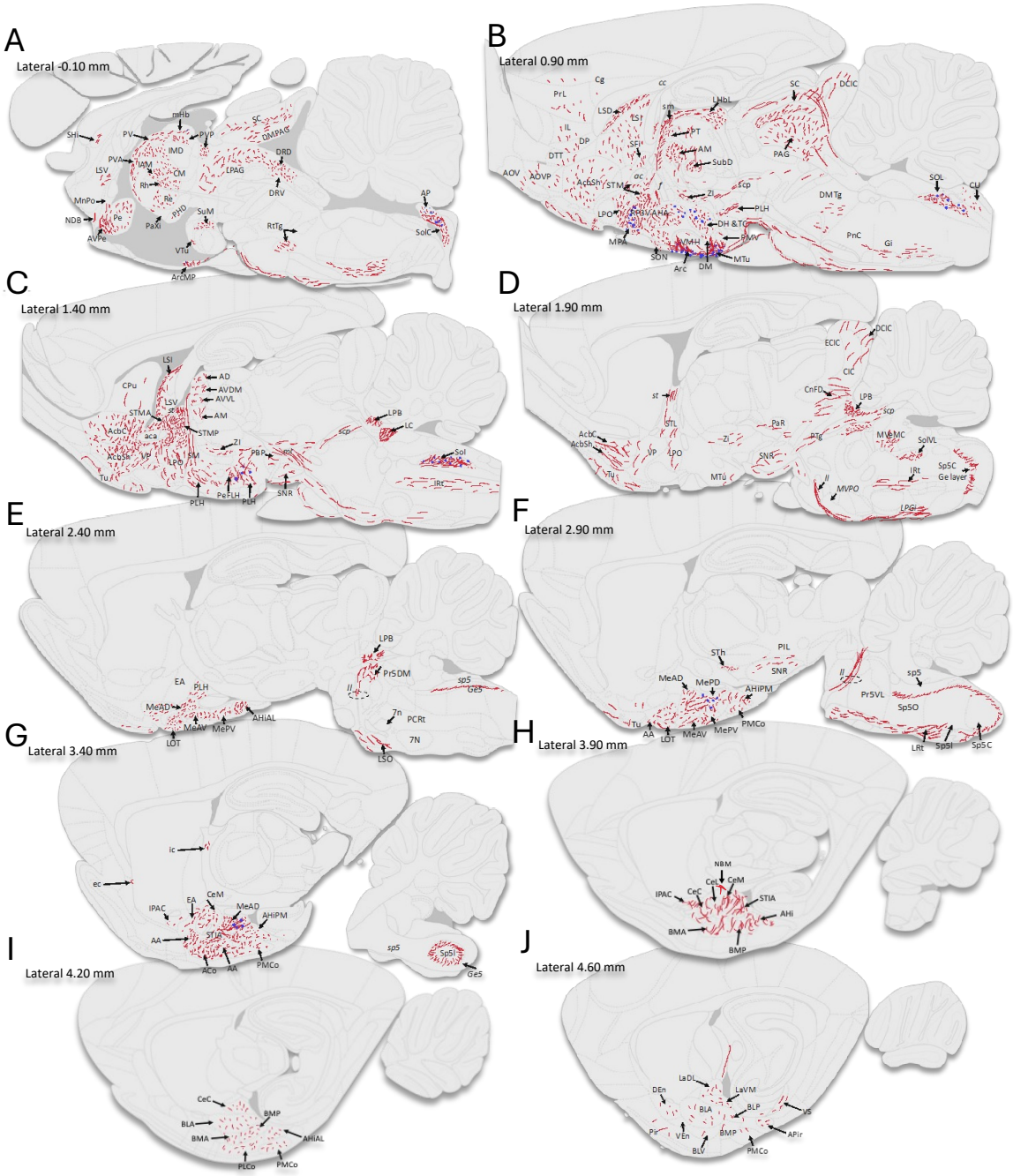

Fig. 3 Mapping of KP immunoreactive fibers and cell bodies ***in rat brain*** *in ten septo-temporal planes based on microscopic observations. Blue dots represent KP-ir cell bodies and red lines represent KP-ir fibers. Relevant anatomical regions have supporting photomicrographs form IHC-DAB reactions using the GQ2 anti-kisspeptin antibody. See table 1 for abbreviations.*

2.2 Detailed description of regional distribution of KP fibers with an emphasis on sensory processing and behavioral state control

The distribution of kisspeptin fibers in several regions involving numerous crucial central sensory relays and behavioral-state control structures suggests wider participation of this peptide in other functions besides its known participation in reproduction and energy balance. In the following sections, we describe these regions in detail.

2.2.1 Telencephalon

In rodent telencephalon, the most prominent KP fiber expressing regions are located in the *lateral septal region* in male and female mice and rats. The strongest expression was observed in the dorsal lateral septal nucleus (LSD) (Fig. 1 A & A2, Fig. 2 B-D, and Fig 3 B-C*),* followed by ventral LS (LSV) (Fig. 2 C, and 3 C). LS is involved in the integration of sensory and emotional information, and can modulate the activity of other brain regions involved in the regulation of behavioral states, such as the hypothalamus, amygdala and hippocampus [20, 21]. Recent studies have reported that the main afferents of the above regions are the subdivisions of the hippocampal formation and the main efferent regions of the LSD are the ventral tegmental area and the supramammilary nucleus, whereas the LSV project mainly to the medial hypothalamic area and medial preoptic area [21]. Activity of lateral septum can lead to changes in behavioral state, including increased exploratory behavioral, social interactions and decreased anxiety, particularly in response to social and emotional stimuli. These changes were reported from clinical studies with KP infusion in human subjects [22]. LS is also a key player for arousal and wakefulness, as well as for regulating processes related to mood and motivation through its extensive connections with numerous regions such as the hippocampus, amygdala, hypothalamus and with the mesocorticolimbic dopamine system [23].

The *medial septum* (MS) also contained mild and sparse innervation in rats and mice (Fig. 1 A and 2 B). This structure is crucially involved in regulating the hippocampal oscillations [24, 25], and recent studies have shown that the medial septum acts as a neural hub that regulates theta oscillations and locomotion speed, influencing goal-directed behaviors such as spatial navigation [26]. Other behaviours influenced by the medial septum include sleep, attention, learning and memory, motivation and emotional processing [27-29].

Sparse fibers were found in *septofimbrial nucleus* (Fig. 3 B) which is an important source of cholinergic inputs to the hippocampus, the entorhinal cortex, influencing hippocampal plasticity and learning and memory under emotional stimuli; and the septohippocampal (SHi, Fig. 2 B) nuclei that provide important GABAergic inputs to hippocampus playing a role in the generation of hippocampal theta oscillation [30]. The above two regions are described for the first time in this study.

Similar to Brailoiu et. al [18], we found sparse fibers in the *horizontal and vertical limbs of the nucleus of diagonal band of Broca* (NDB) (Fig. 2 B). The diagonal band of Broca interconnects the

amygdala and the septal area and projects extensively to hippocampus CA2 subfield which is involved in memory retrieval and social functions [31, 32]. It contains the second largest cholinergic neuronal population in the brain (after the nucleus basalis of Meynert) [33]. It is particularly important in the aging of the brain, since the cholinergic neuronal loss in dementias has been commonly observed in human. The influence of KP to brain cholinergic system is under-investigated.

The presence of kisspeptin fibers in the *nucleus accumbens,* in both core and shell divisions (AcbC and AcbSh), with a mild density in mice and a moderate density in rats (Table 1, Fig. 2 A and 3 B-D) was a remarkable finding of this study. AcbC receives inputs from the prefrontal cortex, the amygdala, and the ventral tegmental area (VTA), which is a key component of the brain reward system. The AcbC integrates these inputs to evaluate the salience and value of rewards and thus helps to regulate motivated behavior. The nucleus accumbens shell is an important brain region involved in the processing of reward-related information and the regulation of motivated behavior, including food intake, drug seeking, and social behavior [34].

Sparse fibers were observed in the *caudate putamen* (CPu Fig. 2 D & 3 C), ventral pallidus (VP, Fig. 3 D), the *sustantia innominata* (SI), as well as main fiber pathways such as *the internal capsule* (ic) and *external capsule* (ec)

In telencephalic *neocortical regions*, we found sparse fibers distributed through the *dorsal tenia tecta* (DTT) and the *dorsal peduncular* (DP), *prelimbic* (PrL) , *infralimbic* (IL), and *cingular* (Cg) cortices, regions that have not been reported in the Brailou study. The observed fibers were mainly located in layers 2/3, and no differences between species were observed (Table 1 and Fig. 2 A & 3 B). The *prelimbic* (PrL), *infralimbic* (IL) and *cingulate cortices* (Cg) have been classically considered to be involved in mediating the role of context in the expression of fear or reward induced behaviors [35] [36, 37]. The DTT and the DP have been classically involved in olfactory information processing, and recently these two structures have been shown to send inputs with information related to psychosocial stress to the dorsomedial hypothalamus, where a cardiovascular and thermogenic sympathetic stress response can be integrated [38]. In other areas classically related to the processing of olfactory information, such as the *ventral and ventroposterior* of the *anterior olfactory nucleus*, (AOV and AOVP) and the *olfactory tubercle* (Tu), we found sparse fibers only in the rat (Tab. 1, Fig. 3 B-D).

In the *amygdalar complex*, we confirmed the KP-ir+ cell population mainly confined within the *medial amygdala's postero-dorsal division* (MePD) which has been reported already elsewhere [39, 40] (Tab. 1 & Figs. 1 C-D, 2 F-G and 3 F-G). Kisspeptin immunolabelled neurons in the MePD and an axon terminal process were observed to innervate the adjacent nucleus of the stria terminalis intra-amygdaloid division and the stria terminalis. Also, we observed KP expressing somas in the septo-hippocampal (SHi) and septo-fimbrial (SFi) region surrounding the anterior commissure, and extending into the septum, these neurons were characterized neurochemically in mice in our previous report [1].

In relation to density of fibers in the septo-bed nucleus of stria terminalis complex, regions with a moderate/intense density of fibers were found within the septal part of the *bed nucleus of the stria terminalis* (BSTMA, BSTMP, BSTLV and BSTLP, Fig. 1 A; Fig. 2 B-D and Fig. 3 B-C). The *temporal intra-amygdala division of the BST* (BSTIA, Fig. 1 C; Fig. 2 F and Fig. 3 H) showed a selective expression of KP fibers. Other regions in the extended amygdala that also showed mild expression of KP fibers were the central amygdalar nucleus (CeC and CeM Fig. 3 G-H) and the medial amygdalar nucleus (MePD and MePV Fig. 2, F-G and 3. G-H). Sparse fibers were found in the *oval nucleus of the stria terminalis* (BSTLD), the *basolateral amygdala* (BLA), the *basomedial amygdala* (BMA), the *lateral part of the central amygdalar nucleus* (CeL), the *cortico-amygdala* (CoA) the *nucleus of the lateral olfactory tract* (NLOT) and the *stria terminalis* (*st*, Fig. 1 C). Compared with the study of Brailou et al, here we report the presence of fibers in the anterior, medial, and cortical amygdala and the intra-amygdaloid division of the stria terminalis (Tab. 2).

2.2.2. Diencephalon

The *hypothalamus* is the region where four of the seven KP neuronal populations have been reported recently by our group, i.e. the rostral periventricular (RP3V) population mainly located in the *medial preoptic area* (MPO), and in the *anteroventral periventricular area* (AVPe) , the arcuate (Arc) population, the dorsomedial hypothalamus (DMH) and the ventral premammillary nu. (PMV) (Fig. 1A; Fig. 2 C,D,F,G,H and Fig. 3 B). After a careful analysis of immunoreacted serial sections, following the pathways of the labelled fibers, we identified some extrahypothalamic regions targets of these regions. Ascending fibers originated in the RP3V population, travel lateral-dorsal-caudally toward the *stria medularis* (*sm*), and the *stria terminalis* (*st*) conduction systems (Fig. 1, B). In their path, they extensively innervate the *bed nucleus of the stria terminalis* (Tab. 2). It is worth noting the presence of KP fibers innervating the border between the *medial (MHb) and lateral (LHb) habenula* (Fig. 2, F-G and Fig. 3 B), it is known that the main input to the habenula is the stria medularis (*sm*). Other fibers originating in the MPO/AVPV region travel to innervate the *organum vasculosum of the lamina terminalis* (OVLT) and then ascend dorsally and laterally to innervate the *accumbens core* (AcbC) and the *lateral septum* regions.

We observed moderately high densities of KP-ir fibers (see Tab. 2) in the caudal periventricular area and ventral periventricular areas of the *arcuate nucleus* (Arc, Fig. 1 E, and Fig. 2 F-H). Some targets of the KP neural population in the *posterior hypothalamus* were identified by following the labelled axon in serially collected sections in coronal and parasagittal planes Some fibers originating in the Arc travelled in the base of the brain reaching the *internal capsule* (*ic*) and *optic tract* through which they travel in a path to the *subthalamic nucleus* (STh), the lateral part of the *supramammillary nucleus* (SuML) and continuing to the *central nucleus of the amygdala* (CeA). Some efferent fibers traveled caudally to innervate the ventral premammillary nucleus (VPM), the *ventral tuberomammillary nucleus* (VTu) the *supramammillary nucleus* (SuM). Some additional fibers surrounded the ventromedial hypothalamus (VMH) and travelled dorsally to innervate the anterior hypothalamic area and continued to innervate medial nuclei of the thalamus including the paraventricular thalamic (PVT) that showed the highest

370 innervation, but also the Intermedio dorsal (IMD) the centro medial (CM), medio dorsal (MD), paratenial
371 (PT), rheuniens (Re) and rhomboid (Rh) nuclei of the thalamus.
372
373 The population of weakly KP immunopositive cells scattered in the *medio-lateral dorsal*
374 *hypothalamic area* (DH) spanning from the posterior part of the *anterior hypothalamus* (AHp) to the
375 posterior hypothalamus (PH), centered in the *tuber-cinerum area* (TC) (Fig. 1 F; Fig. 2 F-H, and Fig. 3
376 B) were observed to project to immediately located *zona incerta* (ZI). Finally, the last population of KP
377 neurons in the PMV was very weakly labelled and it was not possible to identify the axonal projections.
378
379 Other relevant regions in the hypothalamus with KP fibers presence are the *median preoptic*
380 *nucleus* (MPO), the *parastriatal nucleus* (PS), the *paraventricular nucleus medial magnocellular division*
381 (PVNmm) and the *parvocellular division* (PVNmp), and in rat also in the ventral *premammillary nucleus*
382 (PMV) and *ventral tuberomammillary nucleus* (VTu) and *suprammamilary nucleus* (SuM). A mild density
383 of fibers was observed in *dorsomedial hypothalamic nucleus*, MPO , lateral preoptic area, the
384 *periventricular hypothalamic nucleus anterior* (PVa), and the *supraoptic nucleus* (SO). Sparse fibers were
385 found in the *dorsal hypothalamus* (DH), *zona incerta* (ZI), *lateral hypothalamic area* (LH), *posterior*
386 *hypothalamic area* (PH), *retrochiasmatic area* (RCh), and *ventromedial hypothalamic nucleus* (VMH).
387 The KP system in the hypothalamus has been extensively discussed in the literature [(12)].
388
389 In the *thalamus*, the highest density of fibers was observed in the *paraventricular thalamic nucleus*
390 (PVT) in rats and mice (Fig. 1 B; Fig. 2 E-F and 3 B). Mild fibers densities were also observed in other
391 nuclei of the thalamus, such as in the *centromedial* (CM), *mediodorsal* (MD), *paratenial* (PT), *reuniens*
392 (Re), and *rhomboid* (Rh). The epithalamic *habenular nucleus* (Hb) showed a moderate density of fibers
393 mainly located in the border between its medial and lateral subdivisions (Fig. 2 F-G and 3 B), some of
394 these fibers were observed arriving trough the stria medullaris.
395
396 *2.2.3. Mesencephalon*
397
398 Within the mesencephalon, Brailoiu et al [(18)] reported a sparse number of kisspeptin-
399 immunoreactive fibers only in the *dorsomedial periaqueductal gray substance* (DMPAG). In our study
400 that region had the highest density of kisspeptin fibers within the mesencephalon (Fig. 2 J and Fig. 3 B).
401 However, we also visualized a small number of fibers in the *central nucleus of the inferior colliculus* (CIC,
402 Fig. 2 I and Fig. 3 D), *dorsal raphe nucleus* (DR, Fig. 2 J and Fig. 3, A), and sparse fibers in the *deep*
403 *mesencephalic nucleus* (DpMe), *interpeduncular nucleus* (IP), *median raphe nucleus* (MnR), *substantia*
404 *nigra* (SN), *intermediate and deep gray layer of the superior colliculus* (DpG), *supramammillary nucleus*
405 (Sum), *substantia nigra pars reticulata* (SNpr) and *ventral tegmental area* (VTA). The funtional
406 implications for those Kp projections are unknown.
407
408 *2.2.4. Metencephalon and myelencephalon*
409

410 In the metencephalon and myelencephalon, we observed kisspeptin immunopositive somas in the
411 *nucleus tractus solitarius* (NTS or Sol), and *area postrema* (AP) Fig. 1 G; Fig. 2 L and Fig. 3 A-D). We
412 did not observed immunopositive neurons in the caudoventrolateral or the lateral reticular nuclei (CVL
413 and LRt), nor the spinal trigeminal tract, as reported in Brailoiu et al [18]. With respect to the density of the
414 fibers, intense (++++) labelling was found in the *lateral parabrachial nucleus* (LPB, Fig. 1H, Fig. 2 K),
415 the *Kolliker-Fuse nucleus* (KF Fig. 2 K), *NTS*, (Fig. 1 G; Fig. 2 L and Fig. 3 A-D) in the dorsomedial part
416 of the *principal sensorial component of the trigeminal nucleus* (Pr5DM, Fig. 1 K and Fig 3 D-G) and
417 locus coeruleus (Fig. 1 I; Fig 2 K and Fig. 3C). The rat brain also showed intense Kp labeling in the
418 gelatinous layer and the spinal nerve 5 (Fig. 1 J-K and Fig 3 E-F). Moderate (+++) density was observed
419 in the superior cerebral peduncle. Low (++) intensity staining was observed in several nuclei of the
420 reticular formation, including the caudoventral reticular nucleus (CVL); the gigantocellular reticular
421 nucleus (Gi); the intermediate reticular nucleus, the lateral reticular nucleus (LRt); the medullary dorsal
422 reticular nucleus (MdD), the parvicellular reticular nucleus (PCRt) and the rostroventrolateral reticular
423 nucleus (RVL). Sparse (+) fibre density was observed in the ambiguus nucleus (Amb); lateral superior
424 olive (LSO); ventral medullary reticular nucleus (MdV); in subregions of the pontine nucleus such as the
425 brachium pontis (bpPn) the reticular oral part (PnO) and the reticular caudal part (PnC); in the raphe
426 magnus (RMg), obscurus (Rob), pallidus (RPa).
427
428 <u>2.3 Gonadectomy's long term effect on kisspeptin-expressing systems in old rodents: abolition of the</u>
429 <u>GNX's effect after 12 months in most brain areas</u>
430
431 Numerous studies have reported that gonadal status exerts key feedback to KP expression with the
432 neurons of ARC being inhibited and those in the rostral hypothalamus being potentiated by gonadal
433 steroids [1, 41-43]. We analyzed the brains of male and female mice that underwent gonadectomy in their
434 young adulthood (10-12 weeks) and were perfused/fixed 12 months later (15 months of age). We
435 examined KP-ir fibers densities aiming to assess if castration early in reproductive life could modify the
436 density of fibers in aged brain, compared with intact subjects of the same age.
437
438 Table 2 is a report of a semiquantitative analysis of 21 regions within the scope of this study. In
439 female subjects, 19 of the 21 regions were found similar in term of density of KP-ir fibers between old
440 intact subjects ("FC" stands for female control) and subjects undewent ovariectomy in young adulthood
441 ("OVX" stands for ovariectomy, 12 months before the perfusion/fixation). The septohypothalamic nucleus
442 showed increased KP-ir fiber density in OVX subjects. This region, beside of hosting *Kiss1/Slc32a1/Ar*
443 expressing neurons [1] (Fig. 1, A and A1), received direct $RP3V^{KP}$ and Arc^{KP} projections showed by Allen
444 Mouse Brain Atlas, in two experiments using Cre-dependent AAV tracing of axonal projections from
445 RP3V and Arc as injection sites in Kiss1-cre mice (mouse.brain-map.org/experiment/show/232311236
446 and mouse.brain-map.org/experiment/show/232310521). Hence, the origin of this increased fiber density
447 is still not clear. In the RP3V and MPO region, the samples from OVX subjects also showed an increased
448 KP immunoreactivity (Fig. 4). This region, beside of hosting a main KP neuronal populations, also
449 receives Arc^{KP} axonal projections demonstrated by the data base of Allen Institute (mouse.brain-
450 map.org/experiment/show/232310521). In male subjects, 18 of the 21 regions found no apparent

differences between intact male subjects ("MC" stands for male control) and orchiectomized subject ("ORX" stands for orchiectomy). Three regions were found having higher densities of KP-ir fibers the ORX group than MC: dorsal hypothalamus (DH, Fig. 4), paraventricular anterior of thalamus (PVA) and tuberomammillary nuclues. Also, in these 3 regions, MC group showed higher densities than the FC group (Fig. 4).

Table 2 KP immunopositive fiber density analysis in regions related to behavioral states in old female and male mice (14-15 mo.) vs. mice 12 mo. post gonadectomy

	FC	OVX	FC vs OVX	MC	ORX	MC vs ORX	FC vs MC
AcbSh	+++	+++	FC ≈ OVX	++	++	MC ≈ ORX	FC > MC
BSTam	+++	+++	FC ≈ OVX	++	++	MC ≈ ORX	FC > MC
DB	+++	+++	FC ≈ OVX	+	++	MC ≈ ORX	FC > MC
DH	+	+	FC ≈ OVX	++	++	MC < ORX	**FC < MC**
LC	++++	++++	FC ≈ OVX	++++	++++	MC ≈ ORX	FC ≈ MC
LSD	+	+	FC ≈ OVX	+	+	MC ≈ ORX	FC ≈MC
MEA	+	+	FC ≈ OVX	+	+	MC ≈ ORX	FC ≈ MC
MS	++	++	FC ≈ OVX	+	+	MC ≈ ORX	FC > MC
NTS	++++	++++	FC ≈ OVX	++++	++++	MC ≈ ORX	FC ≈ MC
PaAP	+++	+++	FC ≈ OVX	++	++	MC ≈ ORX	FC > MC
PBN	++++	++++	FC ≈ OVX	++++	++++	MC ≈ ORX	FC ≈ MC
TM	+	+	FC ≈ OVX	++	++	MC < ORX	**FC < MC**
PMv	+	+	FC ≈ OVX	++	++	MC ≈ ORX	**FC < MC**
PVA	++	++	FC ≈ OVX	+++	++++	MC < ORX	**FC < MC**
PVN	+++	+++	FC ≈ OVX	++	++	MC ≈ ORX	FC > MC
RP3V	+++	++++	FC < OVX	++	++	MC ≈ ORX	FC > MC
AH (adj SCN)	+++	+++	FC ≈ OVX	++	++	MC ≈ ORX	FC > MC
SHy	+++	++++	FC < OVX	++	++	MC ≈ ORX	FC > MC
STIA	+	+	FC ≈ OVX	+	+	MC ≈ ORX	FC ≈ MC
Wall 3V	+++	+++	FC ≈ OVX	+	+	MC ≈ ORX	FC ≈ MC
ROIs adj. (f/st/sm/ac)	++	++	FC ≈ OVX	++	++	MC ≈ ORX	FC > MC

Table 2. Semiquantitative comparison of kisspeptin immunoreactive cell and fiber distribution in KP expressing regions of control vs gonadectomized mice. Since no differences in the direction of changes were observed in male vs female mice the data reflected here is derived from pooled observations form both sexes. n.a.: does not apply. FC: female control (intact 15 mo. old); OVX: 12 mo. post-ovariectomy (15 mo. old); MC: male control (intact 15 mo. old); ORX: 12 mo. post-orchiectomy (15 mo. old); AcbSh, nucleus accumbens share; BSTam, bed nucleus of stria terminalis, anteromedial division; DB, nucleus diagonal band de Broca; DH, dorsal hypothalamus; LC, locus coeruleus; LSD, lateral septal nucleus, dorsal division; MEA, medial amygdala; MS, medial septal nucleus; NTS, nucleus of tract solitary; PaAP, paraventricular nucleus anterior parvocellular division of the hypothalamus; PBN, parabrachial nucleus and pons; TM, tuberomammillary nucleus of the hypothalamus; PMv, premammillary nucleus, ventral subdivision of the hypothalamus; PVA, paraventricular nucleus anterior division of the thalamus; PVN, paraventricular nucleus of the hypothalamus; RP3V, rostro-periventricular complex of third ventricle of the hypothalamus; AH anterior hypothalamic area (adjacent to suprachiasmatic nucleus, SCN); SHy, septo-hypothalamic nucleus; STIA, nucleus of stria terminalis, intra-amygdalar division; Wall 3V, ependymal layer of the 3rd ventricle; ROIs adj. (f/st/sm/ac), regions of interest adjacent to brain conducting system (fornix, f, stria terminalis, st, stria medullaris, sm, anterior commissure, ac).

474
475

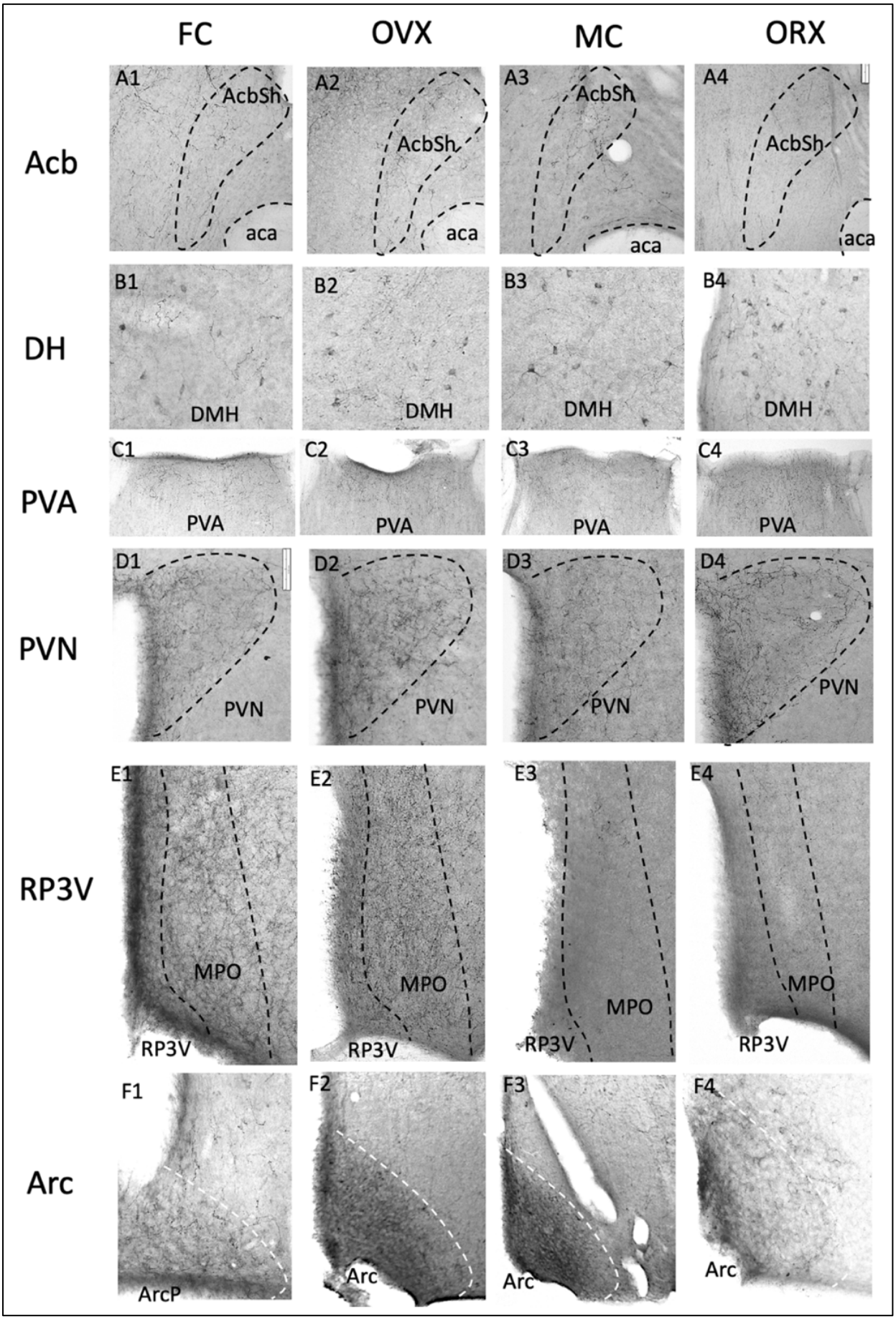
FC
OVX
MC
ORX
Acb
DH
PVA
PVN
RP3V
Arc
A1
AcbSh
aca
A2
AcbSh
aca
A3
AcbSh
aca
A4
AcbSh
aca
B1
DMH
B2
DMH
B3
DMH
B4
DMH
C1
PVA
C2
PVA
C3
PVA
C4
PVA
D1
PVN
D2
PVN
D3
PVN
D4
PVN
E1
MPO
RP3V
E2
MPO
RP3V
E3
MPO
RP3V
E4
MPO
RP3V
F1
ArcP
F2
Arc
F3
Arc
F4
Arc

Fig. 4 Examples of KP-ir fiber density in old mice: comparation of 4 groups. FC: samples from female control, intact mice of 15-month-old; OVX: female mice underwent ovariectomy in young adulthood (3-month-old) and perfused/fixed after 12 months after OVX); MC: male intact mice; ORX: male mice underwent orchiectomy in young adulthood (3 month old) and perfused/fixed after 12 months after ORX).

2.3 Mapping of *Kiss1r and its co-expression with Slc32a1, Slc17a6 and Kiss1* with RNAscope methods suggests the *Kiss1r* is much more widely distributed in the CNS and Kiss1-Kiss1r signaling system can function in *autocrine* and *paracrine* modes

The kisspeptin receptor (Kiss1R), was first identified in rat in 1999 as an orphan receptor, previously termed Gpr54 [44]. Kiss1R is a metabotropic receptor coupled to Gq/11, and its inactivation has been associated with hypogonadism [45]. After kisspeptin binds its receptor, phospholipase C (PLC) is activated and hydrolyzes phosphatidylinositol 4,5-bisphosphate (PIP2) to produce diacylglicerol (DAG) and inositol 1,4,5-trisphosphate (IP3) and the ensuing rise in Ca++ mobilized from intracellular stores and the activation of PKC [46, 47].

There have been few reports on Kiss1R expression in the CNS [46, 48, 49], however, a comprehensive description, especially the Kiss1R co-expression within glutamate-GABA context is incomplete. Using RNAscope dual and multiplex ISH methods, we report here semi-quantitative expression levels of *Kiss1r* in mouse brain sagittal serial sections, in figure 5, based on microscopic observation as different intensities of blue shading. Contrasting with the discrete expression of *Kiss1 in seven neuronal populations* [1], *Kiss1r* expression is widespread and not noticeably restricted to defined nuclei in rodent brain. *Kiss1r* was preferentially expressed in non-GABAergic neurons (Table 3), such as hippocampal projection neurons, main glutamatergic thalamic nuclei, mammillary complex neurons, cerebellar granule cells, and the interposed nucleus. *Kiss1r* was also co-expressed in *Kiss1*-expressing hypothalamic neurons, suggesting an autocrine mechanism for KP signaling. Besides, most neurons neighboring *Kiss1 expressing* cells also expressed *Kiss1r*. These observations suggest that the KP/Kiss1R pathway may use *autocrine* and *paracrine* mechanisms in addition to classical neurotransmission through axon innervation and transmitter co-release, as well as through cerebrospinal fluid (Fig. 1, Panels A3 and E2).

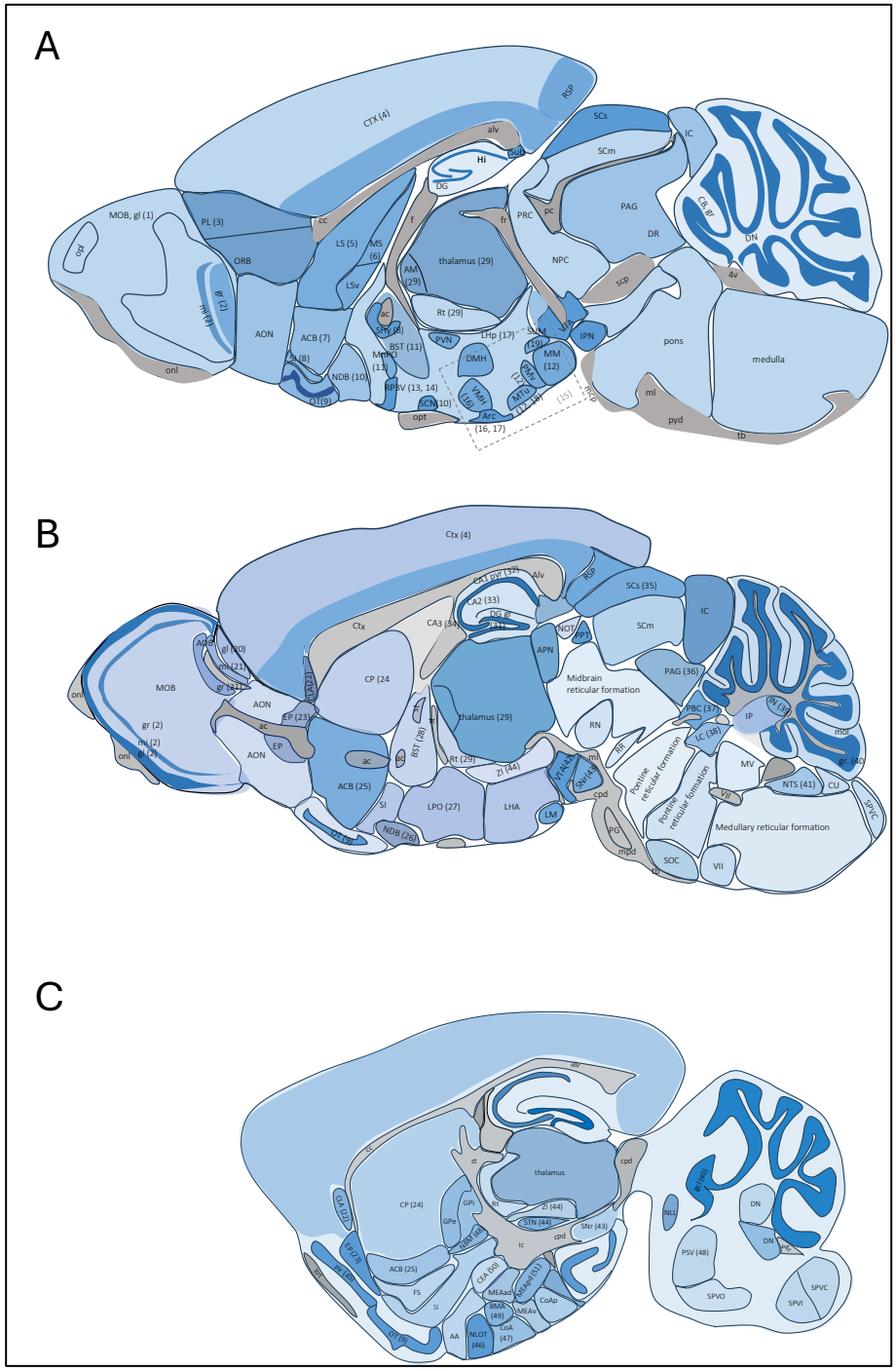

***Fig. 4 Kiss1r* expression assessment in relation to Slc32a1, Slc17a6, Kiss1 expression suggests that the KP-Kiss1R system uses autocrine, paracrine, and neuroendocrine modes for signal transduction.**
(**A–C**) Mapping of *Kiss1*(RNA encoding KP) expression (symbolized by the intensity of blue shading) in three septo-temporal planes in relation to main *Kiss1* containing brain nuclei and subfields, based on microscopic observations. Shaded regions with different blue intensity symbolize the strength of *Kiss1r*. For abbreviations see the corresponding table for abbreviations in table 2.

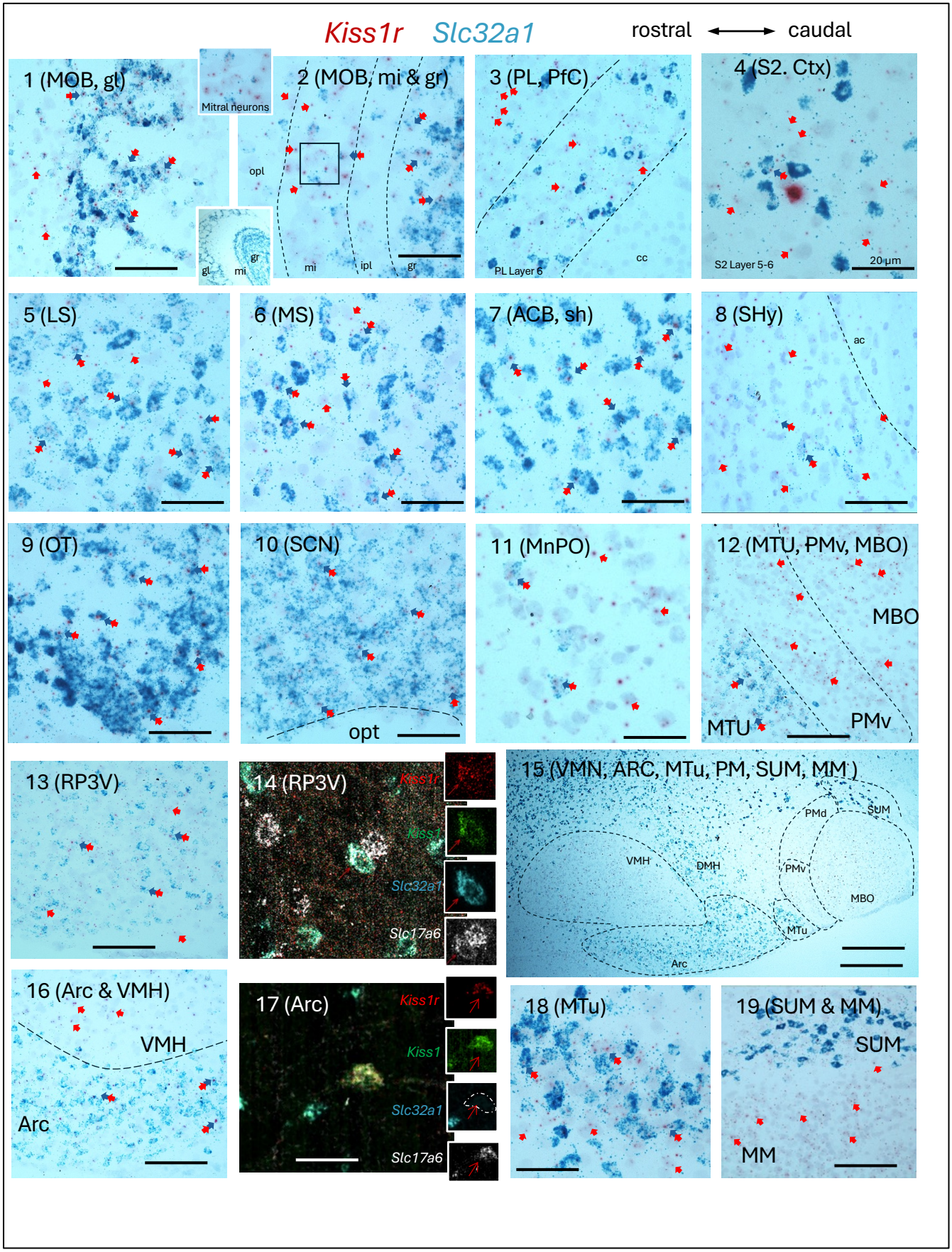
Kiss1r
Slc32a1
rostral
caudal
1 (MOB, gl)
Mitral neurons
2 (MOB, mi & gr)
opl
gl
mi
gr
mi
ipl
gr
3 (PL, PfC)
PL Layer 6
cc
4 (S2. Ctx)
S2 Layer 5-6
20 µm
5 (LS)
6 (MS)
7 (ACB, sh)
8 (SHy)
ac
9 (OT)
10 (SCN)
opt
11 (MnPO)
12 (MTU, PMv, MBO)
MBO
MTU
PMv
13 (RP3V)
14 (RP3V)
Kiss1r
Kiss1
Slc32a1
Slc17a6
15 (VMN, ARC, MTu, PM, SUM, MM)
PMd
SUM
VMH
DMH
PMv
MBO
MTu
Arc
16 (Arc & VMH)
VMH
Arc
17 (Arc)
Kiss1r
Kiss1
Slc32a1
Slc17a6
18 (MTu)
19 (SUM & MM)
SUM
MM

517

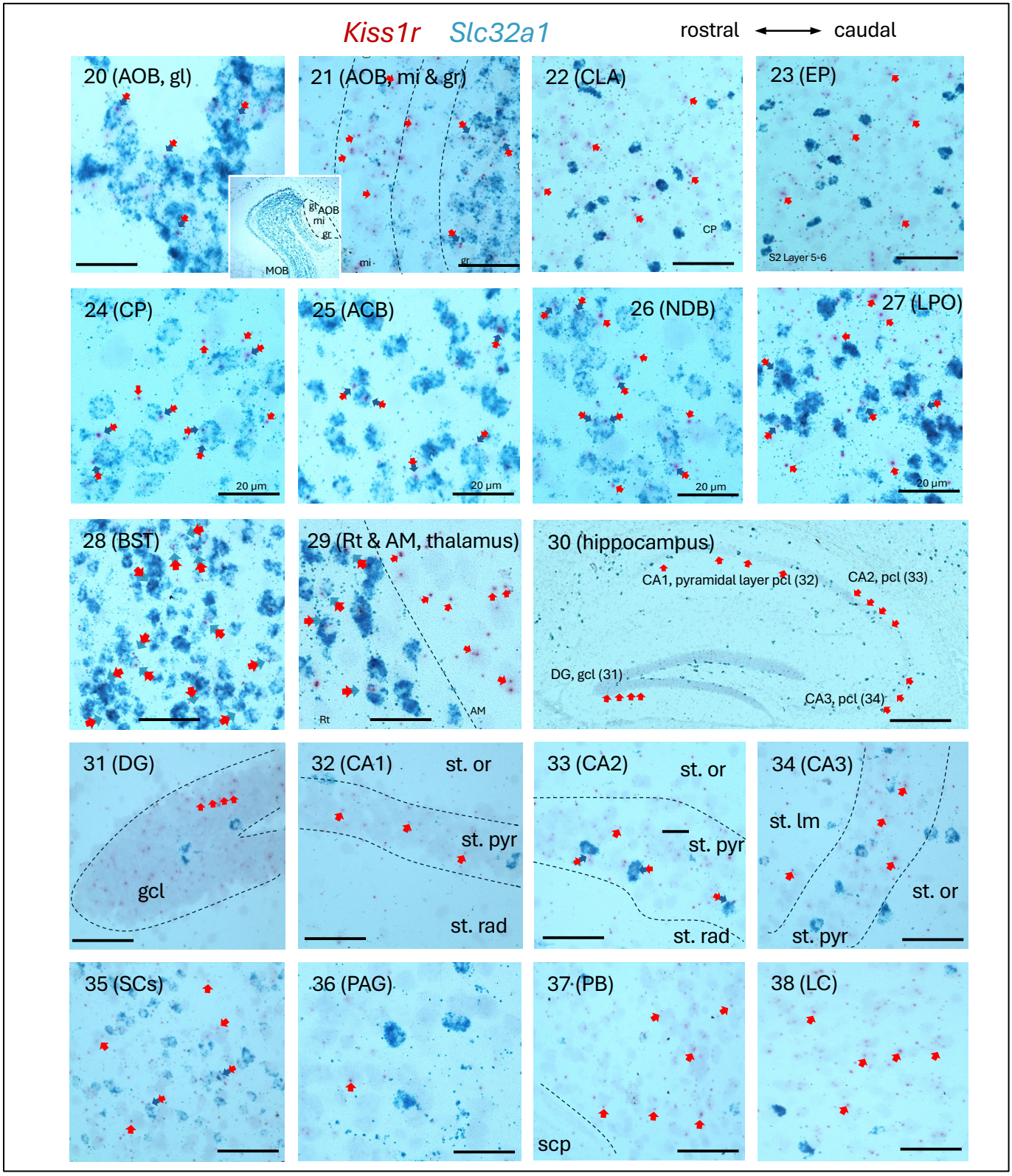
Kiss1r
Slc32a1
rostral
caudal
20 (AOB, gl)
21 (AOB, mi & gr)
22 (CLA)
23 (EP)
gl
AOB
mi
gr
MOB
mi
gr
CP
S2 Layer 5-6
24 (CP)
25 (ACB)
26 (NDB)
27 (LPO)
20 µm
20 µm
20 µm
20 µm
28 (BST)
29 (Rt & AM, thalamus)
30 (hippocampus)
CA1, pyramidal layer pcl (32)
CA2, pcl (33)
DG, gcl (31)
CA3, pcl (34)
Rt
AM
31 (DG)
32 (CA1)
33 (CA2)
34 (CA3)
st. or
st. pyr
st. rad
st. or
st. pyr
st. rad
st. lm
st. or
st. pyr
gcl
35 (SCs)
36 (PAG)
37 (PB)
38 (LC)
scp

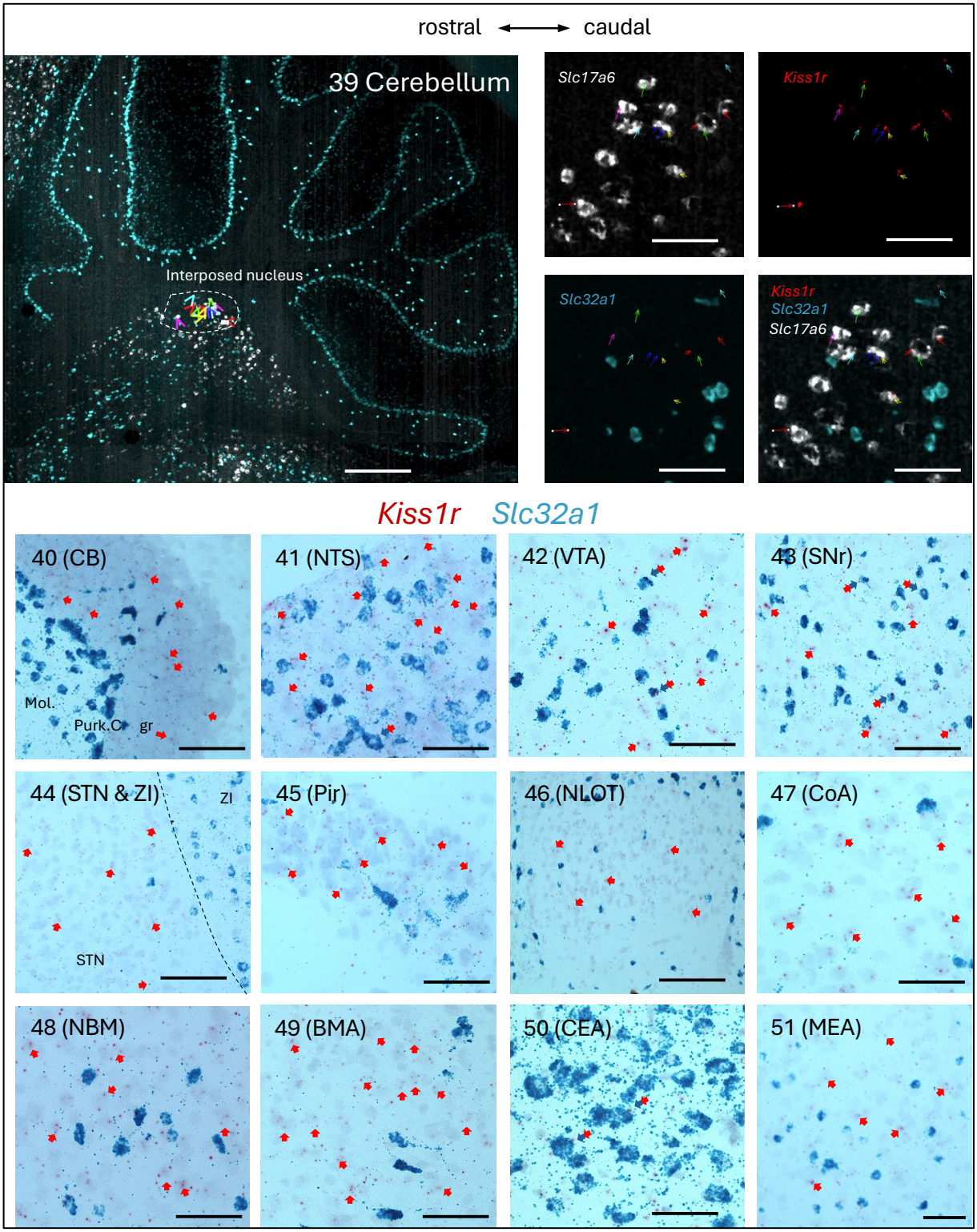

520
521
522
523

Table 2. Distribution, cell types and strength of main ***Kiss1r* expressing cell groups** in mouse brain with comparison of co-expression of ***Slc32a1*** (VGAT)

Cell group / sub-field	Co-expressing Slc17a6 (VGAT)	NO Slc32a1 (VGAT)
Cerebrum: cortical plate		
Olfactory area		
Main Olfactory bulb (MOB)		
Granular cell layer (gr)	+++	+
Inner plexiform layer (ipl)	-	-
Mitral cell layer (mi)	+	+++
Outer plexiform layer (opl)	-	+
Glomerular layer (gl)	+++	+
Accessory olfactory bulb (AOB)	n/r	+
Mitral cell layer (mi)	+	+++
Glomerular layer (gl)	++++	+
Granular layer (gr)	++++	+
Ant olfactory n. (AON)	+	++
Taenia Tecta (TT)	+	++
Piriform area: Pir2	-	+++
Piriform area: Pir3	-	++
N. lat. olfactory tract (NLOT)	-	+++
Cortical amygdalar area (CoA)	-	+++
Hippocampal formation		
dorsal dentate gyrus, granule cells layer (gcl)	+	++++
dorsal hippocampus CA1, pyramidal cell layer (pcl))	+	++++
dorsal hippocampus CA2, pcl	+	++++
dorsal hippocampus CA3, pcl	+	++++
hilus	++	++
Subiculum	++	++
Isocortex		
Layer I	+	++
Layer II-II	+	++
Layer IV	+	++
Layer V	+	++
Layer VI	+	+++
Agranular insular cortex	+	++++
Somatomotor areas		
2ry motor area, layer 2-3:	+	++
2ry motor area layer 5:	+	+++
1ry motor area, layer 2-3	+	++
1ry motor area, layer 5	+	++
Agranular insular cortex	+	+++
Orbital frontal cortex (OFC)		
OFC 1	+	++
OFC 2/3	+	+++
OFC 5	+	+++
Prefrontal Cortex (PFC)		
Ant cingulate cortex (ACC):		
ACC 2/3:	+	+++
ACC 5:	++	+++
Prelimbic (PL)		
PL 2/3	+	+++
PL 5	++	+++
Infralimbic (IL)		
IL 2/3	++	+++
IL 5	++	+++
Prim somatosensory a. SSp,		
SSp 1	+	++
SSp 2/3	+	++
SSp 4 (mouth)	+	++
SSp 5	+	++
SSp 6a	+	+++
Gustatory areas (GU)	+	++
Auditory area	+	++
Visual area	+	++
Visceral area (VISC)	+	++
Temporal association area	+	+++
Ectorhinal area	+	+++
Perirhinal area	+	++
Retrosplenial area	+	+++
Post parietal association area	+	+++
Cortical subplate		
Claustrum	+	++
Endopiriform nucleus	+	++
Lateral amygdalar nucleus (LA)	+	+++
Post amygdalar nucleus (PA)	+	+++
Basomedial amygdala (BMA)	+	+++
Basolateral amygdala (BLA)	+	+++
Cerebral nuclei		
Striatum		
Caudado putamen	+++	+
Lateral septal nucleus (LS)	++	++
Septalhypothalamic nucleus (SHy)	+++	+++
Anterior amygdala area (AAA)	++	+
Central amygdalar nucleus (CEA)	++	+
Medial amygdalar nucleus (MEA)	++	+
Pallidum (basal forebrain)		
Medial Septal nucleus (MS)	++	++
Bed nucleus of stria terminalis (BNST)	++	++
Nucleus basalis of Meyner	+	+++
Globus pallidus	+	++
Substantia innominata (SI)	+	++
Nucleus of diagonal band of Broca (NDB)	+	++
Nucleus Accumbens	++	+
Brain stem, inter-brain		
Thalamus		
Somato-motor related		
Subparafacicular nucleus, magnocellular part	-	+++
Subparafacicular area	-	+++
Peripeduncular nucleus	-	+++
Medial geniculate complex	-	+++
Polymodal association cortex related		
Lat. posterior n. thal	-	+++
Post. limiting nucleus	-	+++
Suprageniculate n.	-	+++
Anterodorsal n.	-	+++
Anteromedial n.	-	++
Parataenial n.	-	++
Intermedial n.	-	+++
Laterodorsal n.	-	+++
Centrolateral n	-	+++
Intermediodorsal n.	-	+++
Mediodorsal n.	-	+++
Pariventricular n.	-	+++
Parateanial n.	-	+++
N. of reuniens[n2]	-	+++
Posterior pretectal n.	-	+++
Precommissural n.	-	+++
Reticular nucleus of the thalamus (Rt)	+++	-
Epithalamus		
Medial habenula	-	++++
Lateral habenula	+	++++
Hypothalamus		
Paraventricular n (PVN)	+	++
Arcuate Nucleus	+++	-
Suprachiasmatic nucleus	+++	+
Rostro-periventricular of the 3V (RP3V)	+++	++
Anterodorsal preoptic n.	++	++
Anteroventral n.	+++	++
Dorsomedial n.	+++	++
Median preoptic n.	++	++
Medial preoptic area	++	++
Vascular organ of lamina terminalis	-	-
Lateral preoptic area (LPO)	++	+
Anterior hyp. area (AH)	+++	+
Premammilary n. (PM)	-	+++++
Lateral mammillary n.	-	+++++
Medial mammillary n. (MM)	-	+++++
Supramammillary n.(SUM)	++	++
Median preoptic n. (MnPO)	+	+++
Lateral hyp. area (LH)	++	++
Subthalamic nucleus (STN)	-	+++++
Retrochiasmatic area	+++	++

Tuberomammilary nucleus (TM, magnocellular subnucleus MTu)	+++	+++
Zona incerta (ZI)	++	+
Ventromedial hyp. n (VMH)	-	+++++
Post. hypothalamic n.	+	+
Midbrain		
Superior colliculus, sensorial (SCS)	+	+++
Superior colliculus, motor (SCM)	+	++
Inf. Colliculus (IC)	++	++
N. of the brachium of IC (BIC)	+	+
Ventral tegmental area (VTA)	+	+++
Sustantia nigra reticulata	+	+++
Midbrain reticular n.	+	++
Periaqueductal gray	++	+++
Midbrain raphe nuclei	+	+++
Pedunculopontine n.	+	++
Dorsal n. raphe	++	++
Pons		
N. lateral lemniscus	+	+
Principal sensorial nucleus of trigeminal nerve	-	++
Koelliker-Fuse subnucleus	-	++
Parabrachial n. lateral div.	-	+++
Superior olivary comp (lat)	-	++
Tegmental reticular n.	++	+++
Dorsal tegmental n.	++	+++
Pontine gray	-	++++
Pontine central gray	++	+++
Supratrigeminal nucleus	++	++
Locus Coeruleus (state)	-	++++
Laterodorsal tegmental n.	++	+++
Pontine reticular n.	++	+++

Superior central n. raphe	++	++
Medulla		
N. tractus solitarii medial	+	+++
N. tractus solitarii lateral	+	+++
Hypoglossal (XII) n.	+	++
Dorsal motor n. of the Vagus nerve (X)	+	+++
Dorsal cochlear n.	-	++
Ventral cochlear n.	-	++
Spinal n. trigeminal	+	++
N. prepositus	-	+++
Facial motor n. (VII)	++	++
N. ambiguus	++	+++
Magnocellular reticular n.	++	+++
Spinal vestibular n.	+++	++
N. X	+	++
N. raphe magnus (state related)	+	+++
N. raphe pallidus (state related)	+	+++
N. raphe obscurus (state rel.)	+	+++
Cuneate n.	+	+
Inferior olivary	+	+++
Cerebellar cortex		
Purkinje's cells	-	-
Golgi's cells	+	-
Granule cells[n4]	-	++++
Cerebellar nuclei		
Interposed n.	+	+
Dentate n.	-	++
Fastigial n.	+	++

* Semiquantitative annotations are used here (the percentage of expressing cell/total Nissl stained nuclei: "-", not detectable; "+", weak (<20%); "++", low (40%-20%); "+++", moderate (60%-40%); "++++", intense (80%-60%); "+++++", very intense (>80%).
** Functional neuroanatomy order and annotations are based on Allen Institute Mouse Reference Atlas.

3. General discussion and conclusions

In this study, we provide a comprehensive description of the distribution of kisspeptin (KP) fibers and cell bodies throughout the brain, as well as the distribution of the Kiss1 receptor (Kiss1R) using GABAergic neuronal groups as markers for regional chemoarchitecture. Our findings were obtained using immunohistochemistry with a highly specific antibody and an improved method that maximized the visualization of KP immunoreactivity. Additionally, we employed a sensitive dual in situ hybridization technique (RNAscope dual and multiplex) to further delineate the expression patterns. Our immunohistochemical analysis revealed a stronger and more extensive distribution of KP immunoreactivity throughout the mouse and rat brains than previously reported.

The distribution patterns suggest that many hypothalamic and extrahypothalamic regions are as strongly innervated as the classical hypothalamic regions known for regulating the hypothalamic-pituitary-gonadal (HPG) axis, but likely serve non-reproductive functions. Indeed, many of these regions are critical for regulating brain states, including telencephalic cortical areas, septal regions (SHy, MS, LS), diencephalic structures (MnPO, SCh, BST, NBM), midbrain regions (PAG, DR, SN/VTA), and metencephalic areas such as the raphe, reticular formation, and LC.

Another prominent finding was the profuse innervation of KP-immunoreactive fibers in regions involved in sensory processing, including the main and accessory olfactory bulbs, olfactory cortical regions, superior colliculus, solitary tract, trigeminal sensory regions, and several thalamic nuclei. A highlight of this study is the analysis of brains from male and female mice that underwent gonadectomy

565 at 3 months of age, with tissue collection occurring one year post-surgery. Notably, the KP fiber density
566 in 21 regions involved in non-reproductive functions was similar or even increased in gonadectomized
567 animals compared to controls, suggesting that the KP system remains functional in other processes beyond
568 reproductive senescence.
569
570 Regarding the distribution of Kiss1r, we observed its preferential expression in non-GABAergic
571 cells, including hippocampal projection neurons, major glutamatergic thalamic nuclei, mammillary
572 complex neurons, cerebellar granule cells, and the interposed nucleus. Additionally, Kiss1r was expressed
573 in Kiss1-expressing hypothalamic cells, indicating a potential autocrine/paracrine role for the peptide.
574
575 The widespread expression of Kiss1r in regions associated with sensory and behavioral state
576 functions, along with the presence of kisspeptin-immunopositive fibers beyond the hypothalamus,
577 suggests a broader and less understood role for kisspeptin signaling in the brain. Recent technological
578 advancements in molecular mapping and imaging have enabled a more systematic examination of Kiss1r
579 distribution and its interaction with kisspeptin fibers throughout the brain. This study aims to bridge this
580 knowledge gap by providing a comprehensive map of Kiss1r expression and kisspeptin fiber distribution
581 in the mouse brain, offering insights into its potential functions within non-reproductive neural circuits.
582
583 We have reported in this study that a high density of KP fibers is present in areas related to pain
584 sensory processing, such as the principal sensorial trigeminal nucleus, the gelatinous layer of the
585 trigeminus and in the periaqueductal gray. In the literature, only a few studies have investigated Kp's role
586 in the modulating of the perception of exteroceptive or interoceptive non-reproductive functions. It has
587 been shown that KP-10 activates calcium signaling pathways in cultured dorsal root ganglion cells,
588 suggesting a possible participation in pain modulation [(50)]. Other regions classically involved in sensory
589 processing have moderate/dense innervation of KP fibers, *i.e.,* superior colliculus for visual processing;
590 the inferior colliculus and superior olive for audition; the parabrachial nucleus and nucleus of the solitary
591 tract (NTS or Sol) for gustatory processing; and the olfactory tubercle, nucleus of the olfactory tract and
592 medial amygdala for olfaction. To our knowledge, the effect of KP on the activity of these regions and its
593 effect on sensory integration has not been studied.
594
595
596 3. Material and methods
597
598 3.1. Animals
599
600 Wistar rats (N=12, male = 6, female = 6) and C57BL/6 mice (N=20, male = 10, female = 10) were
601 obtained from the local animal vivarium and housed three per cage under controlled temperature and
602 illumination (12h/12h) with water and food *ad-libitum*. Mice subjected to gonadectomy were singly
603 housed for recovery for one week after surgery and then returned with their cage mates. All animal
604 procedures were approved by the local research ethics supervision commission (license number CIEFM-
605 079-2020). We analysed two brains sectioned in the parasagittal plane and two brains sectioned in the
606 coronal plane for each sex and species. To evaluate the effect of gonadectomy on the expression of

607 kisspeptin through the brain of male and female mice, we compared the immunoactivity of 4 control vs.
608 4 gonadectomised (one-year post-surgery) mice.
609

610 3.2. Gonadectomy
611

612 *3.2.1 Mouse ovariectomy*
613

614 A dorsal approach to remove the ovaries was used [51]. Briefly, animals were anaesthetised with
615 ketamine 90mg/kg + xylazine 20mg/kg i.p. under anaesthesia animals were placed in ventral recumbency
616 and a 3cm/side squared region centred over the third lumbar vertebra shaved. The shaved area was
617 disinfected with Povidone and 70% alcohol, and a sterile fenestrate drape was placed over it. A single
618 midline dorsal incision approx. 1 cm long was made in the skin at the level of the bottom of the rib cage.
619 The incision was moved laterally to cut the right and left abdominal walls. After cutting the wall (obliques
620 and transverse abdominal muscles), blunt dissection through the body wall with mosquito haemostats was
621 performed. Forceps were gently and carefully introduced to retrieve and exteriorise the corresponding
622 ovary. The ovary, ovarian vessels, and ligament were ligated with 4-0 synthetic absorbable sutures and
623 cut. The wall muscle layers incision was closed with a 4-0 synthetic, monofilament, absorbable suture.
624 The skin incision was closed with a subcuticular suture.
625

626 *2.2.2 Mouse orchiectomy*

627 For the excision of the testicles, we followed a midline incision technique [52]. Briefly, animals
628 were anaesthetised with ketamine 75mg/kg + xylazine 16mg/Kg i.p. and placed on the operating table on
629 their back. The central ventral side of the scrotum area was disinfected with Povidone and 70% alcohol.
630 A single incision on the ventral side of the scrotum (1cm long) penetrating the skin was performed. Each
631 cremaster muscle was cut, and each testis was exposed by gently pulling it through the incision using blunt
632 forceps. Cauda of the epididymis, caput epididymis, vas deferens, and testicular blood vessels were
633 exposed while holding the testicular sack with sterile tooth forceps. A single ligature 4-0 synthetic
634 absorbable suture around the vas deferens and blood vessels was made, prior to excision and gentle
635 removal of the testis. The remaining content was replaced in each one of the testicular sacks. The skin
636 incision was closed with a subcuticular suture.
637

638 3.3 Immunohistochemistry
639

640 Animals were deeply anaesthetised with *i.p.* injected sodium pentobarbital (100mg/kg). They were
641 perfused transaortically with 0.9% saline followed by a cold fixative containing 4% paraformaldehyde in
642 0.1 M sodium phosphate buffer (PB, pH 7.4) plus 15% v/v saturated picric acid for 15 min. Brain tissues
643 were rinsed immediately after the 15 min fixation lapse until the PB yellowish colour was fully cleaned.
644 Brains were then sectioned the same day, using a Leica VT 1000S vibratome at 70µm thickness in the
645 coronal and parasagittal planes and the immunohistochemical (IHC) reaction was performed the same day
646 of the perfusion-fixation. This procedure yielded a more comprehensive IHC labelling than longer fixation
647 and delayed IHC as previously reported and discussed [16]. One of every three sections was selected, and

648 sections from animals that would be compared (*i.e.*, female control *vs.* female gonadectomy) were
649 incubated in the same vial. To block the unspecific antibody binding, sections were incubated for one hour
650 in a solution consisting of 20% normal donkey serum (NDS) diluted in tris-buffered saline (TBS, pH 7.4)
651 plus 0.3% Triton-X (TBST). After the blocking step, sections were incubated for 48h at 4ºC in a polyclonal
652 sheep anti-kisspeptin antibody [15] (GQ2, kindly supplied by Mohammad Ghatei†, Imperial College,
653 London, UK), diluted at a 1:2000 concentration in TBST + 1% NDS. This antibody recognises kisspeptins
654 54, 14,13, and 10 that conserve the C-terminal decapeptide essential for biological activity and shows
655 virtually no cross-reactivity (<0.01%) with other related human RF-amide peptides [15]. After three wash
656 steps, sections were incubated for 24 hours with the secondary donkey anti-sheep biotinylated antibody
657 (Cat: 713-065-147, Jackson ImmunoResearch Inc, PA, USA) diluted at a concentration of 1:500 in TBST
658 + 1% NDS. To detect the biotinylated antibody, VECTASTAIN Elite ABC HRP Kit (Cat: PK-6100,
659 Vector Laboratories, Inc. CA, USA) was used, with H2O2 and 3,3'-Diaminobenzidine as substrates.
660 Finally, sections were mounted on glass slides, dehydrated, dipped in xylene, and cover-slipped using
661 Permount™ mounting medium.
662

663 3.4 Anatomical assessment of kisspeptin innervation density and comparison between control and
664 gonadectomised animals
665

666 To assess the projection patterns of kisspeptin immunopositive fibers through the brain three
667 researchers independently examined the slides under a light microscope, after identifying the regions
668 based on the Paxinos Rat & Mouse brain atlases. Scores of "+" (sparse, main axons passing, without
669 branching nor axon terminals); "++", mild, some branching; "+++", moderate, abundant branching and
670 axon terminals; "++++", intense, extensive branching and intense axon terminals, with confluent fibers
671 that it was difficult to see a separation between them, were reported.
672

673 3.5 Anatomical assessment of mRNA expression in the context of Slc32a1 expressing neurons through
674 the brain.
675

676 The detailed methods have been previously described (Zhang, Hernandez et al., 2018; 2020; 2021). In
677 summary, mice were deeply anesthetized with sodium pentobarbital (Sedalpharma, Mexico, 100 mg/kg
678 b.w., i.p.) and decapitated using a small animal guillotine (Kent Scientific Corp.). The brains were then
679 extracted and rapidly frozen in dry ice. Fresh-frozen brains were sectioned sagittally into 12 µm thick
680 slices using a Leica CM-1520 cryostat and mounted onto positively charged Superfrost Plus microscope
681 slides (Cat. 22-037-246, Fisher Scientific, Pittsburgh, PA).
682

683 Probes used for the detection of mRNAs in the double in-situ hybridization (DISH) were custom-designed
684 by Advanced Cell Diagnostics (https://acdbio.com/rnascope-25-hd-duplex-assay) for kisspeptin receptor
685 (Mm-Kiss1r, channel 2 probe), kisspeptin (Mm-Kiss1, channel 1 probe) and VGAT (Mm-Slc32a, channel
686 2 probe), All experimental procedures were carried out in accordance with the manufacturer's protocol.
687

After sectioning, the slides were fixed in chilled 4% paraformaldehyde (Cat. 30525-89-4, Sigma-Aldrich) prepared in phosphate-buffered saline (Cat. M32631, Sigma-Aldrich), dehydrated in ethanol, and treated with hydrogen peroxide for 15 minutes. They were then treated with protease III for 20 minutes at room temperature, incubated for two hours with the channel 1 and 2 probe mixtures, and underwent amplification and detection steps following the manufacturer's guidelines. Finally, the slides were counterstained with hematoxylin and cover slipped.

Conceptualization: LZ, VSH, MAZ, RPM, LEE; data curation: LZ, VSH, MAZ, ORHP; investigation: LZ, VSH, MAZ, ORHP, RHG; methodology: LZ, VSH, RHG; project administration: LZ, VH, LEE; resources: LZ, LEE, RPM, ICA, RHG; visualization LZ, VSH; writing – original draft: LZ, VH, LEE; review & editing: all the co-authors.

Funding and fellowship acknowledgement

The research leading to these results received funding from the National Autonomous University of Mexico, under Grant Agreement UNAM-PAPIIT-IG200121, Mexican Nacional Council for Humanity, Science and Technology (CONAHCYT), under Grant Agreement CF-2023-243 (LZ), NIMH-IR, NIH, under Grant Agreement MH002386 (LEE). The investigators of this study have been supported by the following fellowships: sabbatical year fellowship from the PASPA program of the Dirección General de Personal Académico (DGAPA) of the Universidad Nacional Autónoma de México (UNAM) (LZ, VSH); Mexican CONAHCYT sabbatical fellowship (LZ) and Fulbright-García Robles Fellowship (VSH), for sabbatical research year in LEE's laboratory of NIMH, NIH; DGAPA-UNAM PREI program for a sabbatical research stay (RPM) in LZ's lab in UNAM, Mexico.

711
712 References
713
714 1. Hernández VS, Zetter MA, Hernández-Pérez O, Hernández-González R, Camacho-Arroyo I, Millar
715 RP, Eiden LE, Zhang L. A comprehensive chemotyping and gonadal regulation of seven kisspeptinergic
716 neuronal populations in the mouse brain. *bioRxiv*. 20242024.07.23.604881.
717 2. Lee JH, Miele ME, Hicks DJ, Phillips KK, Trent JM, Weissman BE, Welch DR. KiSS-1, a novel
718 human malignant melanoma metastasis-suppressor gene. *J Natl Cancer Inst*. 1996; **88**(23): 1731-7.
719 3. Pinilla L, Aguilar E, Dieguez C, Millar RP, Tena-Sempere M. Kisspeptins and reproduction:
720 physiological roles and regulatory mechanisms. *Physiol Rev*. 2012; **92**(3): 1235-316.
721 4. Clarke H, Dhillo WS, Jayasena CN. Comprehensive Review on Kisspeptin and Its Role in
722 Reproductive Disorders. *Endocrinol Metab (Seoul)*. 2015; **30**(2): 124-41.
723 5. Mills EGA, O'Byrne KT, Comninos AN. Kisspeptin as a Behavioral Hormone. *Semin Reprod Med*.
724 2019; **37**(2): 56-63.
725 6. Stephens SBZ, Kauffman AS. Regulation and Possible Functions of Kisspeptin in the Medial
726 Amygdala. *Front Endocrinol (Lausanne)*. 2017; **8**191.
727 7. Liu X, Herbison AE. Kisspeptin Regulation of Neuronal Activity throughout the Central Nervous
728 System. *Endocrinol Metab (Seoul)*. 2016; **31**(2): 193-205.
729 8. Ebrahimi Khonacha S, Janahmadi M, Motamedi F. Kisspeptin-13 Improves Spatial Memory
730 Consolidation and Retrieval against Amyloid-beta Pathology. *Iran J Pharm Res*. 2019; **18**(Suppl1): 169-
731 81.
732 9. Abdul Satar NM, Ogawa S, Parhar IS. Kisspeptin-1 regulates forebrain dopaminergic neurons in
733 the zebrafish. *Sci Rep*. 2020; **10**(1): 19361.
734 10. Sivalingam M, Ogawa S, Parhar IS. Habenula kisspeptin retrieves morphine impaired fear
735 memory in zebrafish. *Sci Rep*. 2020; **10**(1): 19569.
736 11. Clarkson J, d'Anglemont de Tassigny X, Colledge WH, Caraty A, Herbison AE. Distribution of
737 kisspeptin neurones in the adult female mouse brain. *J Neuroendocrinol*. 2009; **21**(8): 673-82.
738 12. Lehman MN, Hileman SM, Goodman RL. Neuroanatomy of the kisspeptin signaling system in
739 mammals: comparative and developmental aspects. *Advances in experimental medicine and biology*.
740 2013; **784**27-62.
741 13. Mikkelsen JD, Simonneaux V. The neuroanatomy of the kisspeptin system in the mammalian
742 brain. *Peptides*. 2009; **30**(1): 26-33.
743 14. Lehman MN, Coolen LM, Steiner RA, Neal-Perry G, Wang L, Moenter SM, Moore AM, Goodman
744 RL, Hwa-Yeo S, Padilla SL, Kauffman AS, Garcia J, Kelly MJ, Clarkson J, Radovick S, Babwah AV, Leon S,
745 Tena-Sempere M, Comninos A, Seminara S, Dhillo WS, Levine J, Terasawa E, Negron A, Herbison AE.
746 The 3(rd) World Conference on Kisspeptin, "Kisspeptin 2017: Brain and Beyond":Unresolved questions,
747 challenges and future directions for the field. *J Neuroendocrinol*. 2018e12600.
748 15. Dhillo WS, Chaudhri OB, Patterson M, Thompson EL, Murphy KG, Badman MK, McGowan BM,
749 Amber V, Patel S, Ghatei MA, Bloom SR. Kisspeptin-54 stimulates the hypothalamic-pituitary gonadal
750 axis in human males. *J Clin Endocrinol Metab*. 2005; **90**(12): 6609-15.
751 16. Zhang L, Hernandez VS. Synaptic innervation to rat hippocampus by vasopressin-immuno-
752 positive fibres from the hypothalamic supraoptic and paraventricular nuclei. *Neuroscience*. 2013;
753 **228**139-62.

754 17. Swanson LW. *Brain Architecture: Understanding the Basic Plan* Oxford, UK: Oxford University
755 Press, 2011.
756 18. Brailoiu GC, Dun SL, Ohsawa M, Yin D, Yang J, Chang JK, Brailoiu E, Dun NJ. KiSS-1 expression
757 and metastin-like immunoreactivity in the rat brain. *J Comp Neurol*. 2005; **481**(3): 314-29.
758 19. Paxinos G, Franklin KBJ. *Paxinos and Franklin's the Mouse Brain in Stereotaxic Coordinates*
759 Elsevier Science, 2012.
760 20. Risold PY, Swanson LW. Connections of the rat lateral septal complex. *Brain research Brain*
761 *research reviews*. 1997; **24**(2-3): 115-95.
762 21. Rizzi-Wise CA, Wang DV. Putting Together Pieces of the Lateral Septum: Multifaceted Functions
763 and Its Neural Pathways. *eNeuro*. 2021; **8**(6).
764 22. Comninos AN, Wall MB, Demetriou L, Shah AJ, Clarke SA, Narayanaswamy S, Nesbitt A, Izzi-
765 Engbeaya C, Prague JK, Abbara A, Ratnasabapathy R, Salem V, Nijher GM, Jayasena CN, Tanner M,
766 Bassett P, Mehta A, Rabiner EA, Honigsperger C, Silva MR, Brandtzaeg OK, Lundanes E, Wilson SR,
767 Brown RC, Thomas SA, Bloom SR, Dhillo WS. Kisspeptin modulates sexual and emotional brain
768 processing in humans. *The Journal of clinical investigation*. 2017; **127**(2): 709-19.
769 23. Sheehan TP, Chambers RA, Russell DS. Regulation of affect by the lateral septum: implications
770 for neuropsychiatry. *Brain research Brain research reviews*. 2004; **46**(1): 71-117.
771 24. Salib M, Joshi A, Katona L, Howarth M, Micklem BR, Somogyi P, Viney TJ. GABAergic Medial
772 Septal Neurons with Low-Rhythmic Firing Innervating the Dentate Gyrus and Hippocampal Area CA3. *J*
773 *Neurosci*. 2019; **39**(23): 4527-49.
774 25. Unal G, Crump MG, Viney TJ, Eltes T, Katona L, Klausberger T, Somogyi P. Spatio-temporal
775 specialization of GABAergic septo-hippocampal neurons for rhythmic network activity. *Brain Struct*
776 *Funct*. 2018; **223**(5): 2409-32.
777 26. Espinosa N, Caneo M, Alonso A, Moran C, Fuentealba P. Optogenetic stimulation of septal
778 somatostatin neurons disrupts locomotory behavior and regulates hippocampus cholinergic theta
779 oscillations. *bioRxiv*. 20222022.09.30.510330.
780 27. Shen L, Zhang GW, Tao C, Seo MB, Zhang NK, Huang JJ, Zhang LI, Tao HW. A bottom-up reward
781 pathway mediated by somatostatin neurons in the medial septum complex underlying appetitive
782 learning. *Nat Commun*. 2022; **13**(1): 1194.
783 28. Srividya R, Mallick HN, Kumar VM. The changes in thermal preference, sleep-wakefulness, body
784 temperature and locomotor activity in the rats with medial septal lesion. *Behav Brain Res*. 2005;
785 **164**(2): 147-55.
786 29. Tsanov M. Speed and Oscillations: Medial Septum Integration of Attention and Navigation.
787 *Frontiers in systems neuroscience*. 2017; **11**67.
788 30. Joshi A, Salib M, Viney TJ, Dupret D, Somogyi P. Behavior-Dependent Activity and Synaptic
789 Organization of Septo-hippocampal GABAergic Neurons Selectively Targeting the Hippocampal CA3
790 Area. *Neuron*. 2017; **96**(6): 1342-57 e5.
791 31. Liu AKL, Lim EJ, Ahmed I, Chang RC, Pearce RKB, Gentleman SM. Review: Revisiting the human
792 cholinergic nucleus of the diagonal band of Broca. *Neuropathol Appl Neurobiol*. 2018; **44**(7): 647-62.
793 32. Dudek SM, Alexander GM, Farris S. Rediscovering area CA2: unique properties and functions.
794 *Nature reviews Neuroscience*. 2016; **17**(2): 89-102.
795 33. Semba K, Fibiger HC. Organization of central cholinergic systems. *Prog Brain Res*. 1989; **79**37-
796 63.

797 34. Floresco SB. The nucleus accumbens: an interface between cognition, emotion, and action.
798 *Annu Rev Psychol*. 2015; **66**25-52.
799 35. Riaz S, Puveendrakumaran P, Khan D, Yoon S, Hamel L, Ito R. Prelimbic and infralimbic cortical
800 inactivations attenuate contextually driven discriminative responding for reward. *Sci Rep*. 2019; **9**(1):
801 3982.
802 36. Capuzzo G, Floresco SB. Prelimbic and Infralimbic Prefrontal Regulation of Active and Inhibitory
803 Avoidance and Reward-Seeking. *J Neurosci*. 2020; **40**(24): 4773-87.
804 37. de Lima MAX, Baldo MVC, Oliveira FA, Canteras NS. The anterior cingulate cortex and its role in
805 controlling contextual fear memory to predatory threats. *Elife*. 2022; **11**.
806 38. Kataoka N, Shima Y, Nakajima K, Nakamura K. A central master driver of psychosocial stress
807 responses in the rat. *Science*. 2020; **367**(6482): 1105-12.
808 39. Gresham R, Li S, Adekunbi DA, Hu M, Li XF, O'Byrne KT. Kisspeptin in the medial amygdala and
809 sexual behavior in male rats. *Neurosci Lett*. 2016; **627**13-7.
810 40. Pineda R, Plaisier F, Millar RP, Ludwig M. Amygdala Kisspeptin Neurons: Putative Mediators of
811 Olfactory Control of the Gonadotropic Axis. *Neuroendocrinology*. 2017; **104**(3): 223-38.
812 41. Starrett JR, Moenter SM. Hypothalamic kisspeptin neurons as potential mediators of estradiol
813 negative and positive feedback. *Peptides*. 2023; **163**170963.
814 42. Rance NE. Menopause and the human hypothalamus: evidence for the role of
815 kisspeptin/neurokinin B neurons in the regulation of estrogen negative feedback. *Peptides*. 2009;
816 **30**(1): 111-22.
817 43. Dubois SL, Acosta-Martinez M, DeJoseph MR, Wolfe A, Radovick S, Boehm U, Urban JH, Levine
818 JE. Positive, but not negative feedback actions of estradiol in adult female mice require estrogen
819 receptor alpha in kisspeptin neurons. *Endocrinology*. 2015; **156**(3): 1111-20.
820 44. Lee DK, Nguyen T, O'Neill GP, Cheng R, Liu Y, Howard AD, Coulombe N, Tan CP, Tang-Nguyen
821 AT, George SR, O'Dowd BF. Discovery of a receptor related to the galanin receptors. *FEBS Lett*. 1999;
822 **446**(1): 103-7.
823 45. Franssen D, Tena-Sempere M. The kisspeptin receptor: A key G-protein-coupled receptor in the
824 control of the reproductive axis. *Best Pract Res Clin Endocrinol Metab*. 2018; **32**(2): 107-23.
825 46. Irwig MS, Fraley GS, Smith JT, Acohido BV, Popa SM, Cunningham MJ, Gottsch ML, Clifton DK,
826 Steiner RA. Kisspeptin activation of gonadotropin releasing hormone neurons and regulation of KiSS-1
827 mRNA in the male rat. *Neuroendocrinology*. 2004; **80**(4): 264-72.
828 47. Ringel MD, Hardy E, Bernet VJ, Burch HB, Schuppert F, Burman KD, Saji M. Metastin receptor is
829 overexpressed in papillary thyroid cancer and activates MAP kinase in thyroid cancer cells. *J Clin*
830 *Endocrinol Metab*. 2002; **87**(5): 2399.
831 48. Herbison AE, de Tassigny X, Doran J, Colledge WH. Distribution and postnatal development of
832 Gpr54 gene expression in mouse brain and gonadotropin-releasing hormone neurons. *Endocrinology*.
833 2010; **151**(1): 312-21.
834 49. Higo S, Honda S, Iijima N, Ozawa H. Mapping of Kisspeptin Receptor mRNA in the Whole Rat
835 Brain and its Co-Localisation with Oxytocin in the Paraventricular Nucleus. *J Neuroendocrinol*. 2016;
836 **28**(4).
837 50. Kelestimur H, Bulut F, Canpolat S, Ozcan M, Ayar A. Kisspeptin leads to calcium signaling in
838 cultured rat dorsal root ganglion neurons. *Gen Physiol Biophys*. 2021; **40**(2): 155-60.
839 51. Stout Steele M, Bennett RA. Clinical Technique: Dorsal Ovariectomy in Rodents. *Journal of*
840 *Exotic Pet Medicine*. 2011; **20**(3): 222-6.

52. Sophocleous A, Idris AI. Ovariectomy/Orchiectomy in Rodents. In: Idris AI, ed. *Bone Research Protocols*. New York, NY: Springer New York 2019: 261-7.

1.